Contrib Mineral Petrol (2013) 166:1099–1118
DOI 10.1007/s00410-013-0911-4

ORIGINAL PAPER

TTG-type plutonic rocks formed in a modern arc batholith by hydrous fractionation in the lower arc crust

Oliver Jagoutz · Max W. Schmidt · Andreas Enggist · Jean-Pierre Burg · Dawood Hamid · Shahid Hussain

Received: 18 June 2012 / Accepted: 15 June 2013 / Published online: 6 July 2013

Abstract We present the geochemistry and intrusion pressures of granitoids from the Kohistan batholith, which represents, together with the intruded volcanic and sedimentary units, the middle and upper arc crust of the Kohistan paleo-island arc. Based on Al-in-hornblende barometry, the batholith records intrusion pressures from ~0.2 GPa in the north (where the volcano-sedimentary cover is intruded) to max. ~0.9 GPa in the southeast. The Al-in-hornblende barometry demonstrates that the Kohistan batholith represents a complete cross section across an arc batholith, reaching from the top at ~8–9 km depth (north) to its bottom at 25–35 km (south-central to southeast). Despite the complete outcropping and accessibility of the entire batholith, there is no observable compositional stratification across the batholith. The geochemical characteristics of the granitoids define three groups. Group 1 is characterized by strongly enriched incompatible elements and unfractionated middle rare earth elements (MREE)/heavy rare earth element patterns (HREE); Group 2 has enriched incompatible element concentrations similar to Group 1 but strongly fractionated MREE/HREE. Group 3 is characterized by only a limited incompatible element enrichment and unfractionated MREE/HREE. The origin of the different groups can be modeled through a relatively hydrous (Group 1 and 2) and of a less hydrous (Group 3) fractional crystallization line from a primitive basaltic parent at different pressures. Appropriate mafic/ultramafic cumulates that explain the chemical characteristics of each group are preserved at the base of the arc. The Kohistan batholith strengthens the conclusion that hydrous fractionation is the most important mechanism to form volumetrically significant amounts of granitoids in arcs. The Kohistan Group 2 granitoids have essentially identical trace element characteristics as Archean tonalite–trondhjemite–granodiorite (TTG) suites. Based on these observations, it is most likely that similar to the Group 2 rocks in the Kohistan arc, TTG gneisses were to a large part formed by hydrous high-pressure differentiation of primitive arc magmas in subduction zones.

Keywords Kohistan batholith · Al-in-hornblende barometry · Magmatic epidote · Granitoid suites · TTG · Island arc · Tectonics

Communicated by T. L. Grove.

Electronic supplementary material The online version of this article (doi:10.1007/s00410-013-0911-4) contains supplementary material, which is available to authorized users.

O. Jagoutz (✉)
Department of Earth, Atmospheric and Planetary Sciences, MIT, 77 Massachusetts Avenue, Cambridge, MA 02139-4307, USA
e-mail: jagoutz@MIT.EDU

M. W. Schmidt · A. Enggist · J.-P. Burg
Department of Earth Sciences, ETH, Sonneggstrasse 5, 8092 Zurich, Switzerland

Present Address:
A. Enggist
Research School of Earth Sciences, The Australian National University, Canberra, ACT 0200, Australia

D. Hamid · S. Hussain
Pakistan Museum of Natural History, Shakarparian, Islamabad 44000, Pakistan

Introduction

The origin of the granitic (s.l.) felsic upper part of the continental crust is now discussed for decades. In general, granitoids encompass a highly diverse suite of rocks

dominated by quartz, plagioclase and alkali-feldspar, and a number of different formation mechanisms and source rocks for different granite types have been proposed. In post-Archean continental crust, the volumetrically dominant granite type is generally metaluminous to slightly peraluminous (A/CNK <1.2) and classically referred to as "I-type" (Chappell and White 1992). These granitoids, mostly granites s.s. and granodiorites (hereafter called GGs), are dominant in subduction-related batholiths such as the Sierra Nevada, Peninsular Range and Gangdese, suggesting a link between subduction zone processes and voluminous I-type granitoid formation. In the Archean, felsic (meta)plutonic rocks are dominated by metaluminous, high Na/K granitoids (tonalites, trondhjemites and granodiorites, the so-called TTG suite), whereas low Na/K GG-types are less common (Condie 1993, 1997; Moyen 2011). Besides their high Na/K characteristics, many, but not all, TTG suites have fractionated middle to heavy rare earth element patterns (MREE/HREE) and other trace element characteristics (e.g., high Sr/Y), indicating the involvement of garnet in their formation.

Consensus exists that strongly peraluminous, so-called S-type granites are formed by partial melting of metasediments (Chappell and White 1992). This interpretation is supported by the Al-rich nature of these granites, their isotopic composition and their often highly heterogeneous zircon populations that may be dominated by >90 % inherited grains. These observations are in line with the generally low melting temperature in pelitic systems with a fluid-saturated minimum melting at 620–650 °C (Thompson and Algor 1977), but also with the fluid-absent melting of muscovite and biotite at ∼<700–800 °C (Vielzeuf and Schmidt 2001).

The origin of the metaluminous GG and TTG "I-type" granites is less certain, as these intrusion suites often have slightly enriched or even mantle-like isotopic compositions. Also, inherited zircons are much less frequent than in S-type granites (Bouilhol et al. 2013). By analogy to S-type granites, it has been proposed that GG and TTG are formed by partial melting of hydrated basaltic rocks (i.e., amphibolites), whereby the melting that results in TTG suites would take place at greater depth compared to that leading to GG suites (Moyen and Stevens 2006). Trace element patterns require the presence of garnet, which stabilizes at ≥10 kbar in basaltic amphibolites (Vielzeuf and Schmidt 2001), and thus, it has been proposed that TTG originates either in thickened lower continental crust (Smithies 2000) or from subducting oceanic lithosphere (Drummond and Defant 1990; Martin 1999). Contrary to pelitic systems, fluid-absent amphibolite melting occurs only at the temperature of ∼850–950 °C (Vielzeuf and Schmidt 2001), posing a thermal problem for widespread lower-crustal melting (Dufek and Bergantz 2005). Apparent support of a partial melting origin of I-type granites comes from fluid-absent partial melting experiments on amphibolites, which produce melt compositions similar to natural granitoids (see review in Moyen and Stevens 2006). Nevertheless, such partial melting experiments can equally be considered as equilibrium crystallization experiments of moderately hydrous melts (Jagoutz and Schmidt 2013).

Indeed, as an alternative to the partial melting hypotheses, I-type granites are interpreted as a product of medium- to high-pressure fractional crystallization starting from subduction-related primitive basaltic mantle melts (see detailed discussion in Jagoutz 2010). Experiments have shown that at elevated pressure and water content, low-Si minerals such as amphibole, garnet and oxide occur early on in the fractionation sequence (Green 1972), pushing derivative liquids over a limited fractionation interval to Si-rich composition producing voluminous amounts of granitic compositions from a basaltic parent (Sisson et al. 2005).

Accordingly, granitoids, including the TTG suite, could equally be formed by derivative liquids resulting from hydrous fractional crystallization of basaltic melts at medium to high pressure (e.g., Jagoutz 2010; Kleinhanns et al. 2003). Interestingly, even though a pressure dependence of the Na concentration of partial melts has been postulated, experimental data indicate that the high Na/K composition of Archean TTG granites cannot be explained by partial melting or fractional crystallization processes at different depths alone (Moyen and Stevens 2006). Instead, the observed high Na/K of TTG suites can only be produced from a high Na/K source (Moyen and Stevens 2006). If the high Na/K in TTGs reflects that of the source, the source composition must have changed in Na/K composition from Archean time to the present day (Jagoutz 2013).

Indeed, granitoids that trace element systematics indicates the involvement of garnet are reported in batholiths build on thick crustal lithosphere (e.g., Gromet and Silver 1987; Lee et al. 2007). Barometric estimates indicate that felsic batholith such as the Sierra Nevada batholith may build to deep crustal levels of ∼30 km (Ague 1997), approaching the stability field of garnet in basaltic to andesitic liquid compositions. Hence, the origin of such granitoids needs to be understood through combining processes in the deep lower crust of thickened lithosphere with those of the upper crust.

This can best be done in the Kohistan arc, exposed in NE Pakistan, where the lower crust records pressures of up to ∼1.5 GPa and where the only complete island arc section is preserved in the geological record (Tahirkheli 1979). In this paper we present field relationships and discuss the chemistry of 90 whole-rock compositions from the Kohistan batholith collected over five field seasons between 2002 and 2008. We provide pressure–temperature

estimates on 37 samples that spatially cover most of the Kohistan batholith. Our results document that the Kohistan batholith was originally 25–30 km thick and that three different groups of granitoids are present with major and trace element characteristics similar to TTG or GG granitoids. We use cumulate compositions from the lower arc crust (Jagoutz et al. 2011) to constrain the origin of these groups.

Geological setting

The Kohistan Island Arc is divided from north to south into three complexes (Fig. 1): (1) the Gilgit Complex, which includes the Kohistan batholith and a volcano-sedimentary cover that is deposited discordantly on the top of the batholithic units (Petterson and Treloar 2004; Petterson and Windley 1985, 1986) but also intruded by the batholith. U–Pb zircon intrusion ages of the batholith range from 110 to 40 Ma (excluding the collision-related leucogranites, for age review see Burg 2011). (2) The mafic/ultramafic Chilas Complex, which is dominated by homogenous gabbronorites with minor associated dunites, pyroxenites, anorthosites and troctolites. These rocks were emplaced during intra-arc rifting and associated decompression melting in the subarc mantle at ~85 Ma (Burg et al. 2006; Jagoutz et al. 2006; Jagoutz et al. 2007; Khan et al. 1989; Schaltegger et al. 2002). (3) The Southern Plutonic Complex (SPC), which includes the Jijal ultramafics composed of dunites, wehrlites, pyroxenites and hornblendites/garnetites overlain by garnet-(meta)gabbros and diorites, the Sarangar gabbro and Kiru intrusive sequence, which, in turn, is overlain by the Kamilla amphibolites (Burg et al. 2005). The SPC represents the deepest exposed arc crust (~1.6–0.8 GPa, Ringuette et al. 1999; Yoshino et al. 1998; for review of geobarometry in the SPC, see Jagoutz and Schmidt 2012). U–Pb zircon intrusion ages of the SPC, mainly determined on leucogranite dikes, are 110–75 Ma (Yamamoto et al. 2005).

The Kohistan batholith has originally been grouped into three stages based on the presence or absence of a gneissic fabric in the granitoids (Petterson and Windley 1985, 1991). In this system, stage 1 plutons show a subsolidus gneissic foliation that has been related to the collision of the Kohistan arc with the Karakoram margin along the Shyok suture. Stage 2 and 3 intrusions do not show subsolidus deformation fabrics and were thought to postdate the collision event. Stage 2 and 3 intrusives are considered to be constituted by subduction-related calc-alkaline granitoids and postcollisional leucocratic anatectic granites, respectively.

However, U–Pb zircon intrusion ages coupled with textural observation do not support the proposed age relationship of plutons based on the presence or absence of deformational fabrics and the interpretation of the timing of emplacement of the stage 1–3 granitoids. Instead, U–Pb zircon ages have shown that no relationship between intrusion ages and presence or absence of a deformational fabric in the rock exists (Jagoutz et al. 2009). Consequently, the strain throughout the batholith was rather heterogeneously distributed, the gneissic fabrics being related to subsequent intrusions of younger magmas, deforming older plutons during emplacement (Jagoutz et al. 2009).

Methods

Mineral analytics

Mineral chemistry was analyzed in standard petrographic thin sections using a JEOL JXA-8200 microprobe at the Institute of Geochemistry and Petrology, ETH. Eleven elements were measured with variable counting times, ranging from 20 (Fe, Mn) to 40 s (Si, Al, Mg, Ca, Na, K, Ti, Cr, Ni) with an acceleration voltage of 15 kV and a beam current of 20 nA. A beam diameter of 3 μm was used to analyze amphibole in order to reduce potential beam damage and associated volatilization or diffusive loss of alkalis during the measurements.

Determination of intrusion pressures

In order to determine the intrusion pressure of the Kohistan batholith granitoids, we used the Al-in-hornblende barometer. The total aluminum content (Al_{tot}) in hornblende and the intrusion pressure are related linearly (Hammarstrom and Zen 1986; Hollister et al. 1987), if plagioclase (andesine to oligoclase), potassic feldspar, biotite, hornblende, titanite, quartz, magnetite or ilmenite and fluid are present in the final stage of crystallization. With a second Fe–Ti-oxide or epidote present in the rock, the f_{O_2} is buffered (Schmidt and Poli 2004; Schmidt and Thompson 1996), and with temperature being almost constant at the H_2O-saturated solidus of granitoid magmas, only the pressure is left as a variable.

The change in Al_{tot} with pressure is mainly attributed to a *tschermak* exchange ($Mg_{-1}Al^{VI}Si_{-1}Al^{IV}$) and to a minor *plagioclase* exchange ($Ca_{-1}Na^{M(4)}Al^{IV}_{-1}Si$), whereas the *edenite* substitution ($NaAl^{IV}Si_{-1}$) is more sensitive to temperature changes (Anderson and Smith 1995; Hammarstrom and Zen 1986; Hollister et al. 1987; Johnson and Rutherford 1989; Schmidt 1992).

Two experimental calibrations of the Al-in-hornblende barometer have been undertaken: (1) Johnson and Rutherford (1989) employing a mixed CO_2–H_2O fluid, thus

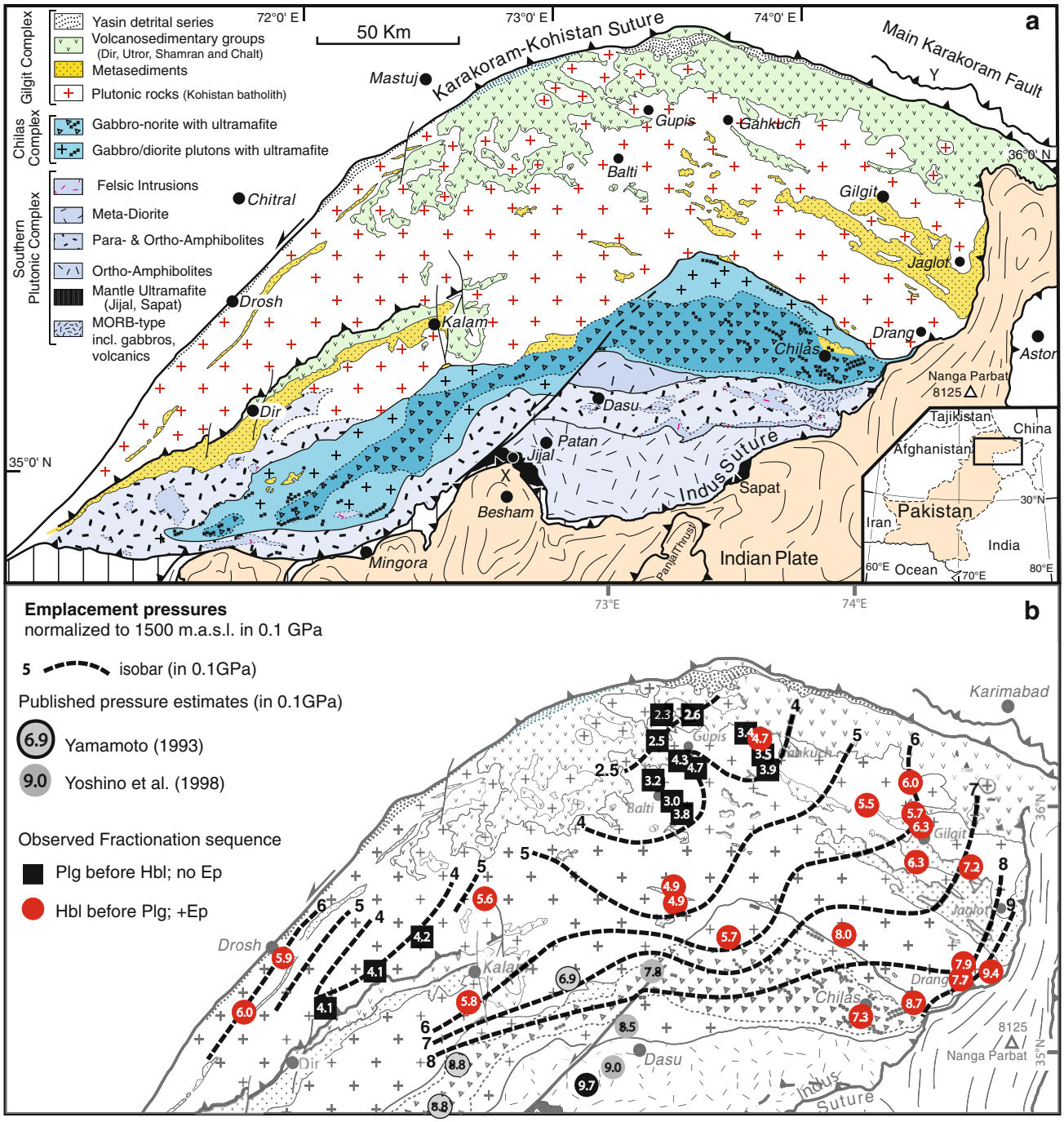

Fig. 1 **a** Geological map of the Kohistan batholith after Jagoutz et al. (2011) showing the sample location and local town names mentioned in the text. **b** Intrusion pressures (in 0.1 GPa = kbar) of the Kohistan batholith constrained by Al-in-hornblende barometry in this study and literature data

shifting phase stability fields and the fluid-saturated solidus to temperatures in the range of 740–780 °C, and (2) Schmidt (1992) under water-saturated conditions in the temperature range of 655–700 °C. Due to the higher temperatures, the former calibration generally yields higher Al_{tot} because of an enhanced *edenite* substitution (Schmidt 1992). The Johnson and Rutherford's (1989) calibration was targeted at extrusives where eruption predates final solidification and where hornblende does not equilibrate down to temperatures of the wet solidus. For intrusives such as the Kohistan batholith, which have no evidence for CO_2-bearing fluids or final equilibration much above the wet solidus, the Schmidt's (1992) calibration is more appropriate. In this study we thus use the following

equation to calculate intrusion pressures: $P_{intrusion}$ (± 0.06 GPa) $= -3.01 + 4.76 \cdot Al_{tot}$, calibrated at pressures ranging from 0.25 to 1.3 GPa (Schmidt 1992).

About 100 granitoids were investigated in thin section to select 37 samples that had the appropriate mineral assemblage described above. Amphibole compositions in these rocks have then been determined by electron microprobe (electronic appendix). For pressure determinations, the rims of hornblende grains that were adjacent to phases or textures forming late in the crystallization sequence, such as orthoclase, quartz and granophyric textures, were measured. This ensures that hornblende was in equilibrium with the near-solidus melt and the hornblende-derived pressures should thus correspond to solidifying pressures. At the same time, very rare rims with secondary actinolitic amphibole were avoided. The hornblende analyses were normalized to 46 charges with a fixed Fe^{3+}/Fe_{tot} ratio of 0.3, which is considered a characteristic for this kind of batholiths. To compensate for varying elevations of the sample locations, differing by 2,200 m, all pressures were normalized to 1,500 m.a.s.l. by assuming a lithostatic pressure gradient of 0.028 GPa/km.

For comparison, we also determined pressures after Anderson and Smith (1995) in conjunction with the *edenite*-thermometer of Holland and Blundy (1994) in order to take possible differences in emplacement temperature into account (Blundy and Holland 1990). We employed the Michel-Lévy method, precise to ± 2 mol%, to optically determine the anorthite content of the plagioclase. Differences in pressures calculated from the Schmidt's (1992) calibration and the Anderson and Smith (1995) fit are small (electronic appendix), indicating that almost all samples equilibrated at the wet solidus. Hence, our geological implications drawn from the pressure determinations are independent of the calibration used.

Absolute pressures calculated using the Al-in-hornblende geobarometer after Schmidt (1992) have errors of ± 0.06 GPa. Relative intrusion pressures between different samples, however, have smaller errors (typically ± 0.02 GPa), their precision being limited by the homogeneity of hornblende rim compositions. Comparison of the Al-in-hornblende geobarometer pressures to thermodynamically calculated pressures from pressure sensitive metamorphic reactions agrees within ± 0.1 GPa with the experimental calibration used in this study (Ague 1997).

Whole-rock major and trace element analyses

Representative rock samples were crushed and then ground in an agate mill to obtain a powder with a grain size of less than 10 μm. These powders were dried at 110 °C and the loss of ignition determined by heating for 2 h at 1,050 °C. The rock powders were then mixed with $Li_2B_4O_7$ (1:5), molten and poured into platinum crucibles to obtain glass discs using a Class M4 fluxer. Major and selected trace elements of the glass discs were analyzed using an X-ray fluorescence spectrometer (WD-XRF, Axios, PANalytical) at the Institute of Geochemistry and Petrology at ETH Zurich. The calibration was based on 30 certified international standards, and relative mean errors are 1 % for major elements.

Trace element concentrations were measured in triplicate using a laser-ablation inductively coupled plasma mass spectrometer at the Institute of Geochemistry and Petrology, ETH. The laser-ablation system consists of a GEOLAS 193-nm ArF-excimer laser and a Perkin Elmer Elan 6100 DRC ICP-Mass Spectrometer. Fragments of whole-rock XRF glass pills were ablated at three locations by the laser. Blank correction was done using a lithium-tetraborate-only pill. The concentration of the samples was obtained using the XRF Al concentration as an internal standard and NIST 610 glass as an external one. Corrections and the calculations of concentrations were done using LAMTRACE (Jackson, version 2.16, 2005) and the three concentrations of each sample averaged.

Results

Field relations and intrusion style

The Kohistan batholith is an intricate complex consisting of multiple plutonic bodies that intruded into plutonic, volcanic and sedimentary sequences (Fig. 1). The field observations reported here refer to outcrop observations in mainly two sections: (1) along the main and a few subsidiary roads from Gupis to Gilgit and (2) along the Karakoram Highway from Gilgit to Chilas including a few tributary roads. In both sections, the batholith is nearly continuously exposed.

The field investigations indicate the presence of two principal end-member styles of intrusion, which, as can be shown by Al-in-hornblende geobarometry, relate to different depths of emplacement. The intrusion styles of the shallower crustal levels in the northern and northwestern part are characterized by larger ($\leq$1 km wide) magmatic bodies, whereas in the southeast, the deeper part of the batholith is characterized by a multitude of typically 10–50-m-wide dikes that indicate the simultaneous presence of multiple magmas and crystal mushes. In the following paragraphs, we describe the intrusion styles that characterize the shallower and the deeper levels of the Kohistan batholith.

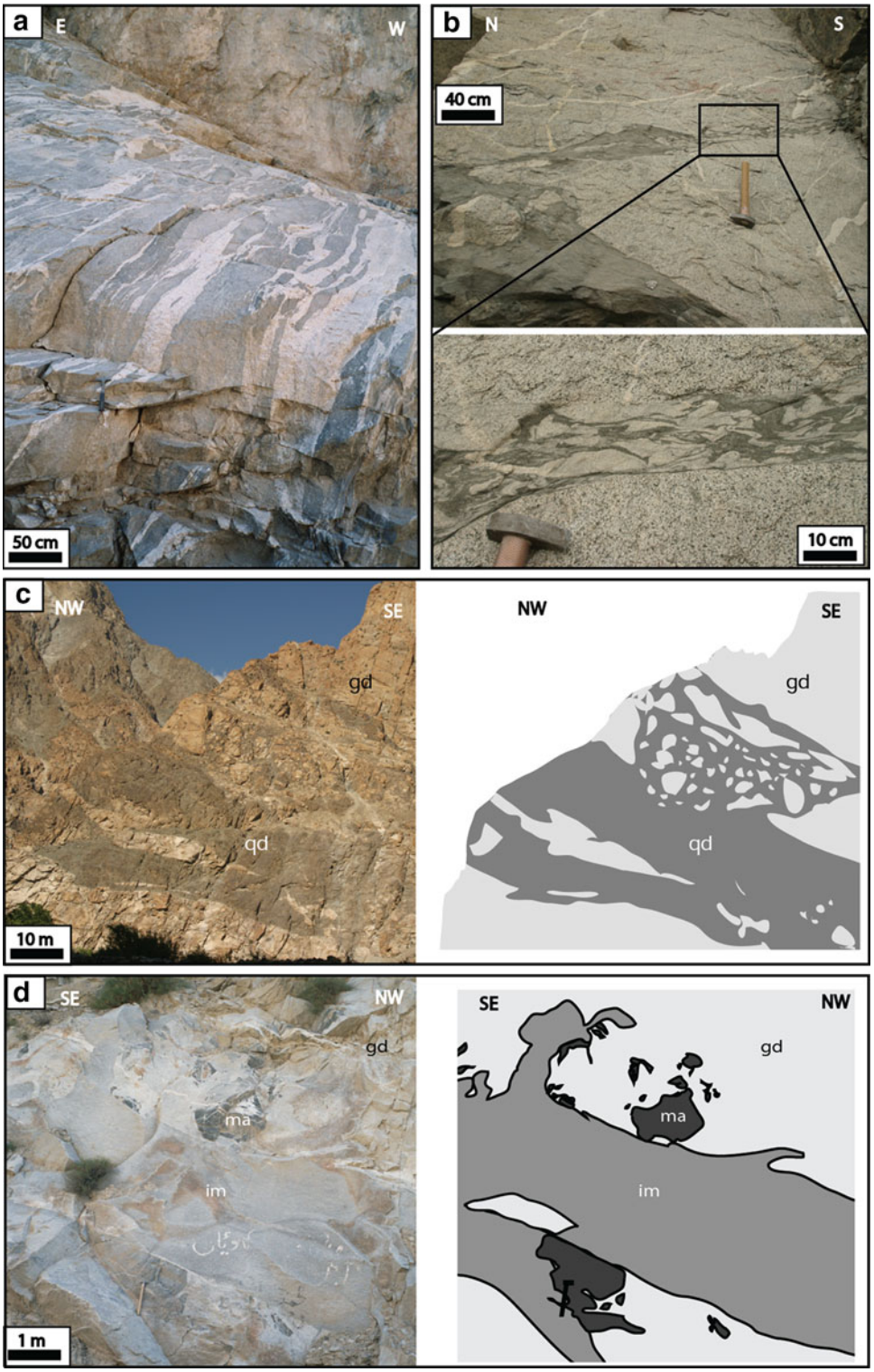

The shallower northern part

In the shallower central and northern area, around Gupis and Gahkuch (Fig. 1), large 100–1,000 m wide, relatively homogenous granitoid stocks and plutons are common. These granitoids are mostly granites and granodiorites, less frequently tonalites and a few monzo- and quartz diorites. The intrusive bodies often display magmatic foliation and flow alignment of feldspars and enclaves. The feldspars and mafic and metasedimentary enclaves, which are

◀**Fig. 2** Field evidence from the shallower level (northern part) of the Kohistan batholith documenting the importance of magma mingling in the shallower plutonic arc crust. **a** Schlieren zone between a quartz dioritic and granitic stock. Approaching the schlieren zone in the field from the east, one observes an increasing abundance of granitic enclaves first and then schlieren in the quartz diorite over ~100 m, followed by the schlieren zone which is roughly 100 m wide and consists of similar proportions of quartz dioritic and granitic schlieren. Granitic schlieren get more, quartz dioritic schlieren less abundant over another 50 m, finally leading to a massive granite body with only minor content of quartz dioritic schlieren in the west. No intermediate composition is developed between the granite and quartz diorite. **b** A quartz dioritic intruded into granodioritic rocks. Toward the right, southern side, the granodiorite fragments start to deform ductile, as more mafic magma intrudes, the mingling propagates along the cracks and fractures. The compositions, however, remain separate and do not mix to form an intermediate composition. **c** Evidence for intrusion of more mafic melts in more felsic composition and associated magma mingling is found at all scale (here large outcrop scale). **d** There are three different magma types involved in this photograph. The *light gray*, medium-grained granodioritic magma (gd) was intruded by the *dark gray* mafic magma (ma). The mafic dyke is dismembered, which is interpreted as the result of cooling of the system producing a more viscous, crystalline mafic melt compared to the silica-richer host that remained longer above the liquidus at lower temperatures. Fragments of the mafic rocks are further transported as enclaves, indicating that the granodioritic magma was still convecting. Finally, a fine-grained, *light gray* dike of a more intermediate composition (im) intrudes and has sharp contacts on the right but shows more diffuse contacts to the *left* in the picture and the contact gets more anastomosing (see *drawing*). All three compositions are interpreted to have coexisted as crystal mushes, yet the intermediate composition resulted not from the mixing of the more mafic and more evolved compositions observed in this outcrop

flattened and elongated, are often oriented parallel to the intrusive boundaries with the surrounding plutons. Contact zones between different intrusive units are often characterized by distinct schlieren zones, indicating that the different magmas were crystal mushes and, thus, contemporaneous. However, sharp contacts indicating temporally separated intrusions are equally common. Schlieren zones are 50–150 m wide (Fig. 2a) and are typically oriented parallel to the contact and decrease in abundance with increasing distance from the contact. Contacts between the different schlieren can be sharp or diffuse on a centimeter scale in the same outcrop. Relatively dark quartz diorite dikes (20–50 m wide) are often dismembered within a stock or pluton of granodioritic to tonalitic composition. No significant field evidence was observed, indicating that mingling magmas of more mafic and felsic compositions mix to form an intermediate homogenous composition (Fig. 2). Few leucogranitic dikes and veins occur that, generally, are not more than 1–3 m wide and show sharp contacts to the host rock occur. In the Balti area, black-colored, holohyalin rhyolitic dikes of decimeter thickness are present and intrude monzodioritic rocks.

Isolated swarms of parallel, fine-grained mafic, tens-of-centimeter-to-meter-thick dikes are common to the west of Gupis and have sharp contacts to the granitoid host plutons. These dikes crosscut the plutonic rocks and contact zones between stocks, implying intrusion of the mafic magma after full crystallization of the host. In the northern central area, i.e., around Gahkuch, sills of granodioritic composition intruded the sediments. Sedimentary fragments, contact metamorphosed to calc-silicates of meter size, were torn off by the intrusion and are partly dissolved in the magma.

The deeper southeastern part

The intrusion style observed in the southeastern, deeper part of the batholith (Gahkuch, Gilgit to Drang, Fig. 1) differs markedly, as individual plutonic bodies are, on average, at least an order of magnitude smaller (1–100 m wide). Most igneous bodies are composed of an interconnected network of 5–20-m-wide dikes with highly variable compositions and mutual crosscutting relationships (Fig. 3). Some contacts are sharp, suggesting near- or subsolidus intrusion, but many contacts are diffuse with local schlieren zones implying interaction between different magma mushes. Magmatic features include magma mingling within veins and dikes of centimeter to meter thickness, intrusion of granodioritic or granitic magmas into quartz dioritic crystal mush (Fig. 3), intrusion of mafic magmas into granodiorites or granites, and basaltic dikes intruding in and becoming dismembered in quartz dioritic to granitic stocks. These observations attest for the contemporaneous occurrence of the full suite of magma compositions as crystal mushes on a local scale (Fig. 3).

At this level of the batholith, fracturing of the host during emplacement of subsequent younger magmas played an important role in the intrusion processes, as observed in the field. Magmas of dioritic, quartz dioritic or granitic composition intrude in-between centimeter-to-meter-scale fragments of quartz dioritic, granodioritic or granitic composition. Fragments often show sharp boundaries to the intruding magma, illustrating an absence of hybridization at this stage. In other situations, the boundaries of rounded fragments are more diffuse or schlieren-like, implying that magma mingling processes took place. Also, composite fragments of hybrid compositions can be found in the various intruding magmas, which, again, have either sharp or diffuse contacts. These observations illustrate that emplacement, fracturing and hybridization processes were multiply repeated during the crustal-forming processes. Furthermore, in contrast to the observations from the shallower northwestern part of the batholith, the mafic magmas in the southeast generally appear to be less viscous during emplacement. Typical magmatic structures are cross-beds and layering due to the settling of dense, mafic minerals during magma flow. Such features are less

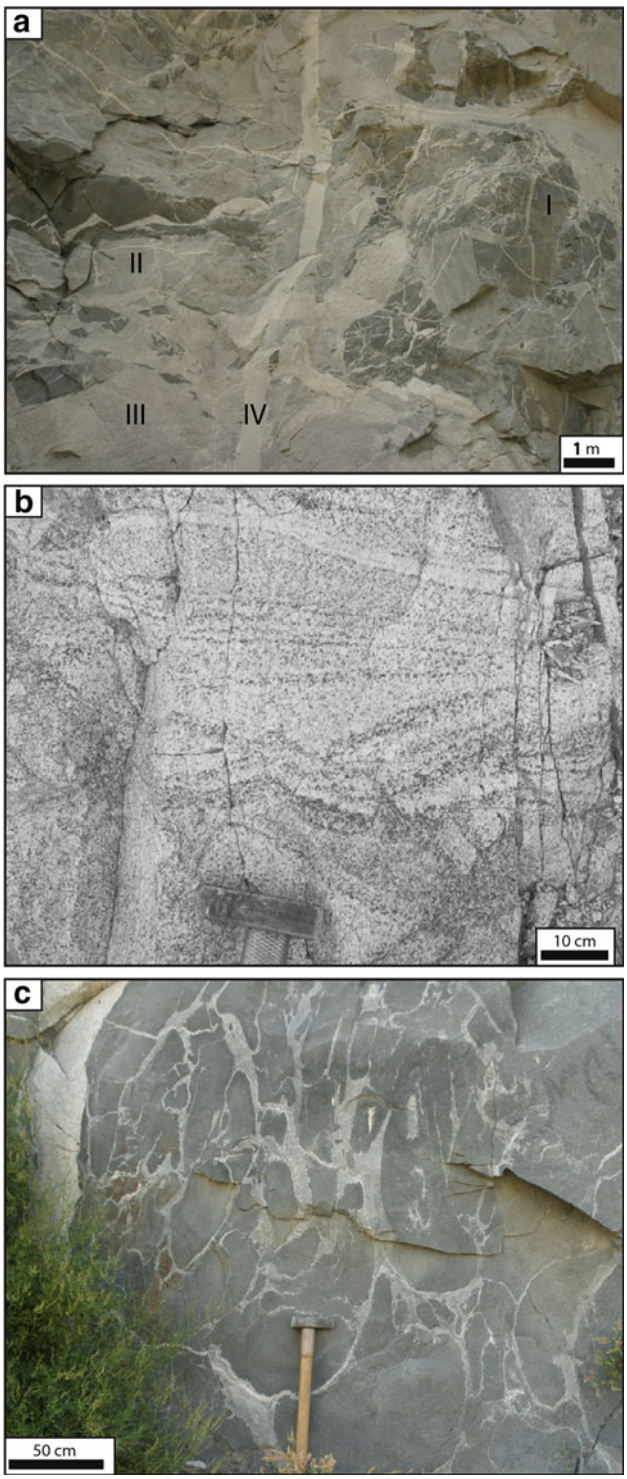

Fig. 3 Field observations from the deeper levels (south western part) of the Kohistan batholith. Similarly to what is shown in Fig. 2, ample evidence for magma mingling is observed, but no evidence is found for large-scale magma mixing: **a** complex outcrop of at least four different compositions (labeled from I–IV with increasing felsic composition). All compositions with the exception of composition (IV) are interpreted to have coexisted as liquid crystal mushes. Indicating complex mingling of magmas of different compositions. However, no homogenous mixed magma is developed between any of the compositions. **b** Magmatic layering within a coarse-grained granodiorite. **c** Chilled pillow of diorite in granitic host

abundant or locally absent in the northern part of the batholith. The above-described intrusion style is somewhat in contrast to the map around Gilgit from Petterson and Windley (1986) who have identified 18 larger bodies of typically 5–10 km in diameter but ranging up to 250 km^2. Re-examination of several of these bodies has revealed their composite nature, i.e., magmatic structures as described above.

The abundance of leucogranite dikes and veins increases strongly eastward toward the Nanga Parbat syntaxis and becomes most prominent near Jaglot, close to the contact with the Indian basement gneisses (Fig. 1). Where leucogranite dikes are abundant, they typically form dike swarms of subparallel orientation. Leucogranite veins vary in thickness from decimeter to meter in width and form a more or less irregular network of interconnected veins near Jaglot. Contacts between leucogranites and host rocks are sharp, indicating intrusion of these granites after the system cooled down significantly and/or at high fluid pressures. This observation is in accordance with U–Pb zircon ages of the leucogranites (~30 Ma, Bouilhol et al. 2013), which are younger than Ar–Ar hornblende and biotite cooling ages of some of the host rocks (~30–40 Ma Treloar et al. 1989) and generally postdate the Kohistan arc-India collision around 50 Ma (Bouilhol et al. 2013). These postcollisional, often peraluminous granitoids are interpreted to result from re-melting of the Indian plate (Bouilhol et al. 2013) and have been excluded from the discussion presented here.

Petrography

All plutonic rocks analyzed are homogeneous, holocrystalline, fine to medium grained and generally fresh. Following the classification of Streckeisen (1974), the sampled rocks are gabbros, diorites, monzodiorites, quartz diorites, quartz monzonites, tonalites, granodiorites and granites. Quartz diorite and granodiorite compositions are dominant in all visited parts of the Kohistan batholith that was estimated to be composed of 5 % mafic rocks (gabbro/diorite), 30 % quartz and quartz monzodiorite, 13 % tonalites, 25 % granodiorites, 12 % I-type granites and 15 % leucogranite dikes and stocks (Petterson and Windley 1985; Jagoutz and Schmidt 2012). In the following, we summarize the textures of the samples used for geobarometry; details for each sample including the modal mineralogy are presented in the electronic appendix.

For the quartz diorites to granites, independently of the rock type, two different crystallization sequences can be distinguished in the field and in thin section, based on the

textural relations of the minerals (Figs. 1, 4): In the northern part of the batholith, magmatic epidote is absent. In this part, hornblende is often interstitial and poikilitic, and plagioclase is devoid of any hornblende inclusions. We interpret this texture to indicate a relatively late occurrence of hornblende in the crystallization sequence, i.e., after the first crystallization of plagioclase. These textural observations define the following crystallization sequence for these rocks:

$$\text{Oxides} \pm \text{Pyroxene(s)} \rightarrow \text{Plagioclase} \rightarrow \text{Hornblende} \rightarrow \text{Biotite} \rightarrow \text{Quartz} \rightarrow \text{Orthoclase} \quad \text{(i)}$$

This sequence indicates the onset of crystallization of each phase. Hornblende, in part, crystallizes concomitantly with plagioclase, which, together with orthoclase, remains stable and crystallizes until the solidus. In the northern central area, near Balti and Gupis in particular, both clino- and ortho-pyroxenes remain as relics in hornblende or are enclosed in biotite, which is less common toward the east. Pyroxene-bearing tonalites were also reported by Nawaz et al. (1987) from the SW of the Kohistan batholith, in the NW of Dir (Fig. 1).

From NW to SE, magmatic epidote first occurs near Gahkuch (Fig. 1) and is present in all rocks further to the south and southeast. In these rocks, euhedral and poikilitic hornblendes are common and plagioclase contains inclusions of euhedral hornblende (Fig. 4). From this texture, we deduce that hornblende begins to crystallize prior to plagioclase. Pyroxene relicts are rare in this part of the batholith and pyroxene, thus is enclosed in brackets in the following crystallization sequence:

$$\text{Oxides}(\pm\text{Pyroxenes}) \rightarrow \text{Hornblende} \rightarrow \text{Plagioclase} \rightarrow \text{Biotite} \pm \text{Epidote} \rightarrow \text{Quartz} \pm \text{Epidote} \rightarrow \text{Orthoclase} \quad \text{(ii)}$$

In some samples epidote appears texturally with biotite, while in others biotite crystallizes clearly before epidote.

Geobarometry

In the north, plutonic rocks stratigraphically just below the volcano-sedimentary cover yield Al-in-hornblende crystallization pressures as low as 0.23 GPa, corresponding to a depth of ~8–9 km (assuming a density of 2,800 kg/m^3) during intrusion (Fig. 1, see also electronic appendix). The stratigraphic thickness in the overlying volcano-sedimentary sequence amounts to ~5 km (Burg 2011), suggesting that a few kilometers are now lacking. In the central northern batholith, calculated pressures increase to the northeast from ~0.30 GPa around Balti to 0.35–0.48 GPa near Gupis (Fig. 1). Crystallization pressures are higher (~0.60 GPa) in the northeastern Gilgit area. At Drang, in the southeast of the batholith, pressures are higher with a maximum of 0.77–0.94 GPa. Pressures calculated on samples collected by Heuberger et al. (2007) near the western limit of the batholith yield ~0.6 GPa, with isobars parallel to the Karakoram-Kohistan suture. About 20 km to the SE, samples from the batholith in the hanging wall of the Dir-Kalam fault intruded at 0.33–0.37 GPa, but pressures are much higher in the footwall of this fault, eastward near Kalam and in the south-central part (0.54–0.57 GPa).

At two locations (near Gahkuch and Drang), samples collected within less than 10 km of each other differ in crystallization pressures by as much as $\Delta P = 0.13 \pm 0.06$ and 0.17 ± 0.09 GPa, respectively. These differences cannot be explained by the uncertainty of the geobarometer itself, as relative pressures are precise to about ±0.02–0.04 GPa; hence, the relative pressure differences of 0.13 and 0.17 GPa in these two locations are robust. Further confirmation of these differences stems from the presence of magmatic epidote in the higher-pressure sample near

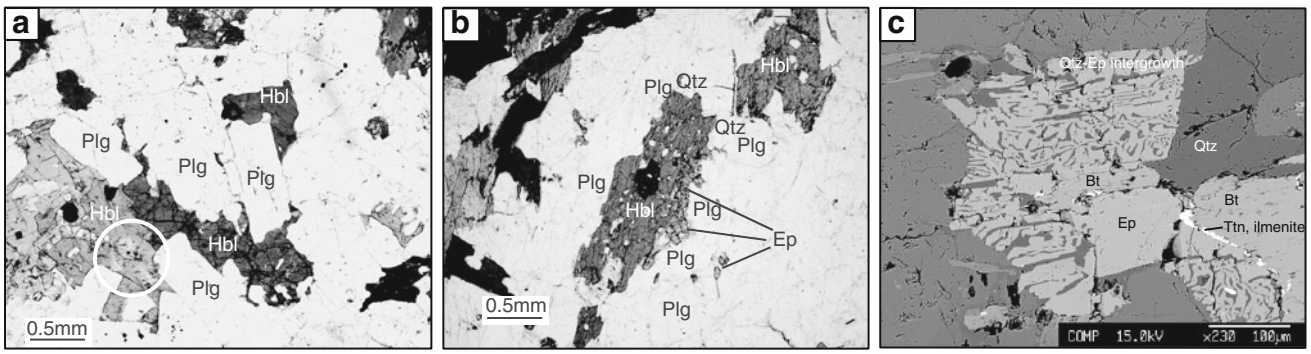

Fig. 4 **a** Thin-section photograph showing interstitial hornblende and euhedral, tabular plagioclase (under plane polarized light). Hornblende is late in the crystallization sequence relative to the plagioclase. The *circle highlights* pyroxene relics in hornblende. **b** Thin-section photograph showing euhedral poikilitic hornblende containing quartz inclusions (under plane polarized light). Plagioclase is euhedral to subhedral, tabular to equant. Hornblende is early in the crystallization sequence relative to the plagioclase. Magmatic epidote is present in this sample. **c** *Backscatter* electron image showing subhedral epidote intergrown with quartz, which is taken as evidence for a magmatic origin. *Bt* biotite, *Ep* epidote, *Hbl* hornblende, *Plg* plagioclase, *Qtz* quartz, *Ttn* titanite

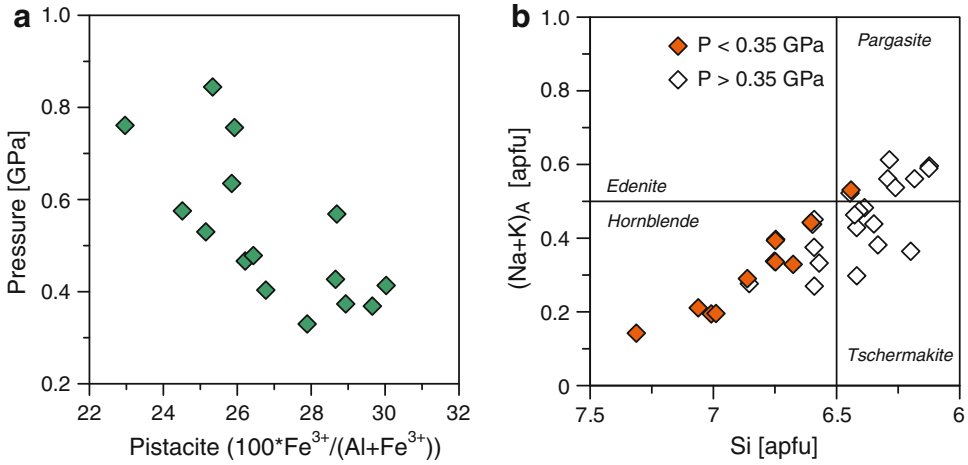

Fig. 5 **a** Pistacite (Ps = Fe^{3+}/(Fe^{3+}+Al)) versus pressure diagram of epidote. Ps component increases with decreasing pressure. **b** Higher-pressure hornblende associated with magmatic epidote and hornblende crystallizing earlier than plagioclase has lower Si content than the lower-pressure amphibole (nomenclature after Leake 1978)

Gahkuch and its absence in the lower-pressure ones. Consequently, these differences should reflect variations in depth with time in a given location. Evidently, the time–depth evolution may go both ways: Batholith construction on the top may lead to increasing pressures with time, while erosion would lead to decreasing pressures with time (see also below).

The calculated pressures correspond well to the two distinct crystallization textures observed. Samples of the northern area, which exhibit plagioclase before hornblende in crystallization sequence (i), equilibrated at shallower levels than samples showing hornblende before plagioclase in crystallization sequence (ii). The transition between the two crystallization sequences is located at ~0.45 GPa, which is consistent with the experimentally determined phase diagrams of granodioritic to tonalitic bulk compositions: At the pressures of >0.4 GPa, hornblende crystallizes at the liquidus or is closer to the liquidus than plagioclase; at lower pressures, plagioclase constitutes the liquidus phase (Green 1982; Lambert and Wyllie 1974; Schmidt and Thompson 1996). In the Kohistan, magmatic epidote is only present in rocks with intrusion pressures ≥0.47 ± 0.06 GPa. As predicted experimentally (Schmidt and Thompson 1996), a decreasing pistacite component in epidote [Ps: Fe^{3+}/(Fe^{3+}+Al)] is observed with increasing pressure (Fig. 5). Amphiboles associated with magmatic epidote in samples that yield high crystallization pressures are mostly hornblendes, whereas those from lower-intrusion-pressure samples tend toward pargasitic compositions (Fig. 5).

Emplacement pressures derived from metamorphic reactions of 0.69 GPa for the southernmost part of the Kohistan batholith (Yamamoto, 1993), of 0.75 GPa north of Dasu, of 0.6–0.7 GPa within the Chilas Complex (Jagoutz et al. 2007) and of 0.90 GPa in the Southern Plutonic Complex (Yoshino et al. 1998) are in accordance with the Al-in-hornblende emplacement pressures at the southern limit of the batholith. Furthermore, they are consistent with the pressure of 0.98 GPa obtained from a coarse-grained pegmatite dike of tonalitic composition in the Southern Plutonic Complex, the dike containing the critical mineral assemblage for the Al-in-hornblende barometer (Fig. 1).

Geochemistry

Based on geochemistry and mineralogical assemblage, most granitoids of the Kohistan batholith belong to a calc-alkaline, I-type suite including diorite, tonalite, granodiorite and granite compositions. Generally, the intrusives are metaluminous to slightly peraluminous (A/CNK <1.1). SiO_2 concentrations range from 50.4 to 76.8 wt%, and X_{Mg} (X_{Mg} = molar MgO/(MgO + FeO_{tot})) generally decreases with increasing SiO_2 from ~0.6 to 0.2. For intermediate compositions, X_{Mg} remains in a narrow range (~0.4–0.5) over a wide range in SiO_2 content, i.e., from 56 to 71 wt%, a typical behavior of calc-alkaline granitoids (Fig. 6). Primitive mantle-normalized trace element patterns (Fig. 7) are generally characterized by an enrichment of the light (LREE) MREE compared to the HREE. The high-field-strength elements (HFSE) Nb and Ta are generally depleted compared to elements of similar incompatibility. These geochemical characteristics are typical for subduction-zone-related magmas (e.g., McCulloch and Gamble 1991) and confirm the overall supra-subduction zone setting of the Kohistan arc (Tahirkheli 1979). Most studied samples are characterized either by the absence of or, when present, by a negative Eu/Eu* (Eu/Eu* = ($2Eu_N$/(Sm_N + Gd_N)) and/or positive Pb anomaly. Very few samples have positive Eu/Eu* anomalies and high Sr/Nd, indicating a cumulative composition due to the accumulation of plagioclase.

In detail, the trace element systematics allows us to separate the granitoids of the Kohistan into three groups (Fig. 7): Most abundant are Group 1 rocks that have weakly fractionated MREE/HREE ($0.6 < Gd/Yb_N < 2.1$),

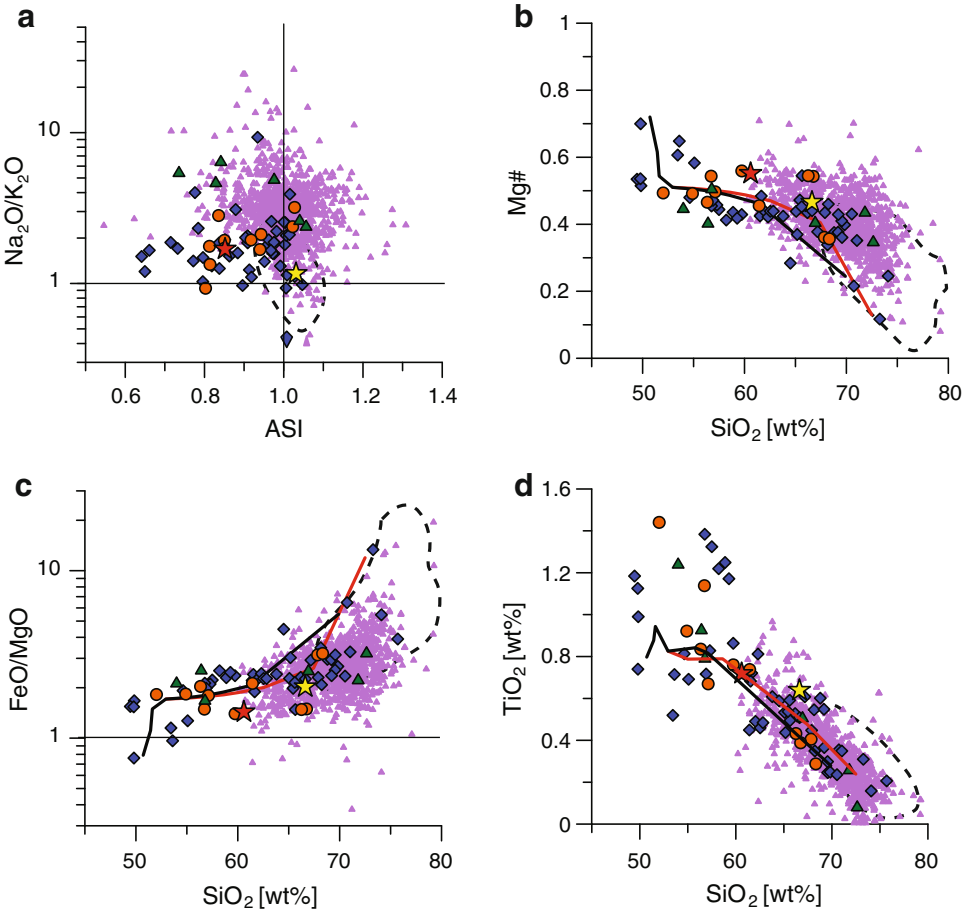

Fig. 6 Major element characteristics of the Kohistan batholith rocks compared to Archean TTG- and GG-type rocks (dashed field indicates compositional range of GG rocks, purple triangle are TTG rocks, grouping and data from Moyen (2011)). Shown is also the LLD model of Jagoutz (2010). *Black line* represents a pure fractional crystallization model, whereas the *red line* includes 5 % assimilation in the lower arc crust (see text and Jagoutz 2010 for details). Colour coding of the symbols relates to the grouping of the rocks based on the trace element data (*blue* Group 1, *orange* Group 2 and *green* Group 3, see text and Fig. 7 for details for grouping). *Yellow* and *red stars* denote the upper and bulk crust composition of Rudnick and Gao (2003), respectively (ASI = molecular ratio $Al_2O_3/(CaO + Na_2O + K_2O)$)

high LREE/MREE ($1.2 < La/Nd_N < 2.9$), a pronounced negative Ti anomaly and generally $(Th/U)_N > 1$. Group 2 is defined by highly fractionated MREE/HREE ($2.1 < Gd/Yb_N < 3.7$), high LREE/MREE ($1.2 < La/Nd_N < 3.1$) and the absence of any Ti anomaly. Group 3 rocks have less fractionated MREE/HREE ($0.9 < Gd/Yb_N < 2.2$), low LREE/MREE ($0.8 < La/Nd_N < 3.3$), a variable (i.e., positive and negative) Ti anomaly and $(Th/U)_N < 1$.

In Figs. 6 and 7, the chemical characteristics of the Kohistan batholith granitoids are compared to Archean GG- and TTG-type rocks following the classification and dataset of Moyen (2011). Archean TTG is characterized by high Na/K ratios of generally 1–4, similar to the range observed in the Kohistan batholith (~0.5–6). Group 1 and 2 granitoids have trace element characteristics strikingly similar to average Archean GG and TTG suites, respectively.

Discussion

The emplacement depth of the Kohistan batholith

The exhumation levels in the central and eastern part of the Gilgit Complex increase from the north to the southeast from ~0.2 to ~0.9 GPa with the highest pressures recorded near the Nanga Parbat syntaxis. Remarkably, the batholith shows very limited large-scale structural disruption. Only toward the west exhumation was accompanied by a major fault zone, the Dir-Kalam fault mapped as a thrust by Sullivan et al. (1993). However, pressures are 0.15 GPa lower in the NW-hanging wall of the fault, compared to the footwall, indicating that at some point in its history, the fault had some significant normal movements. In the NW block, pressures then increase toward the northwest, where the Shyok suture records a dominant strike-slip motion. In fact, the map of Fig. 1 results in surprisingly consistent pressures given the fact that the batholith was constructed essentially on its own substrate over 70 Ma. Unfortunately, 4D information where time and pressure could be correlated is lacking.

A spatial relationship similar to the intrusion pressures has been observed for the Ar–Ar cooling ages within the Gilgit Complex, where Ar–Ar ages become progressively younger toward the Nanga Parbat syntaxis. The Ar–Ar pattern is thought to reflect the influence of the syntaxis on the exhumation of the Gilgit Complex (Treloar et al. 1989), and our data corroborate that the greatest uplift in the

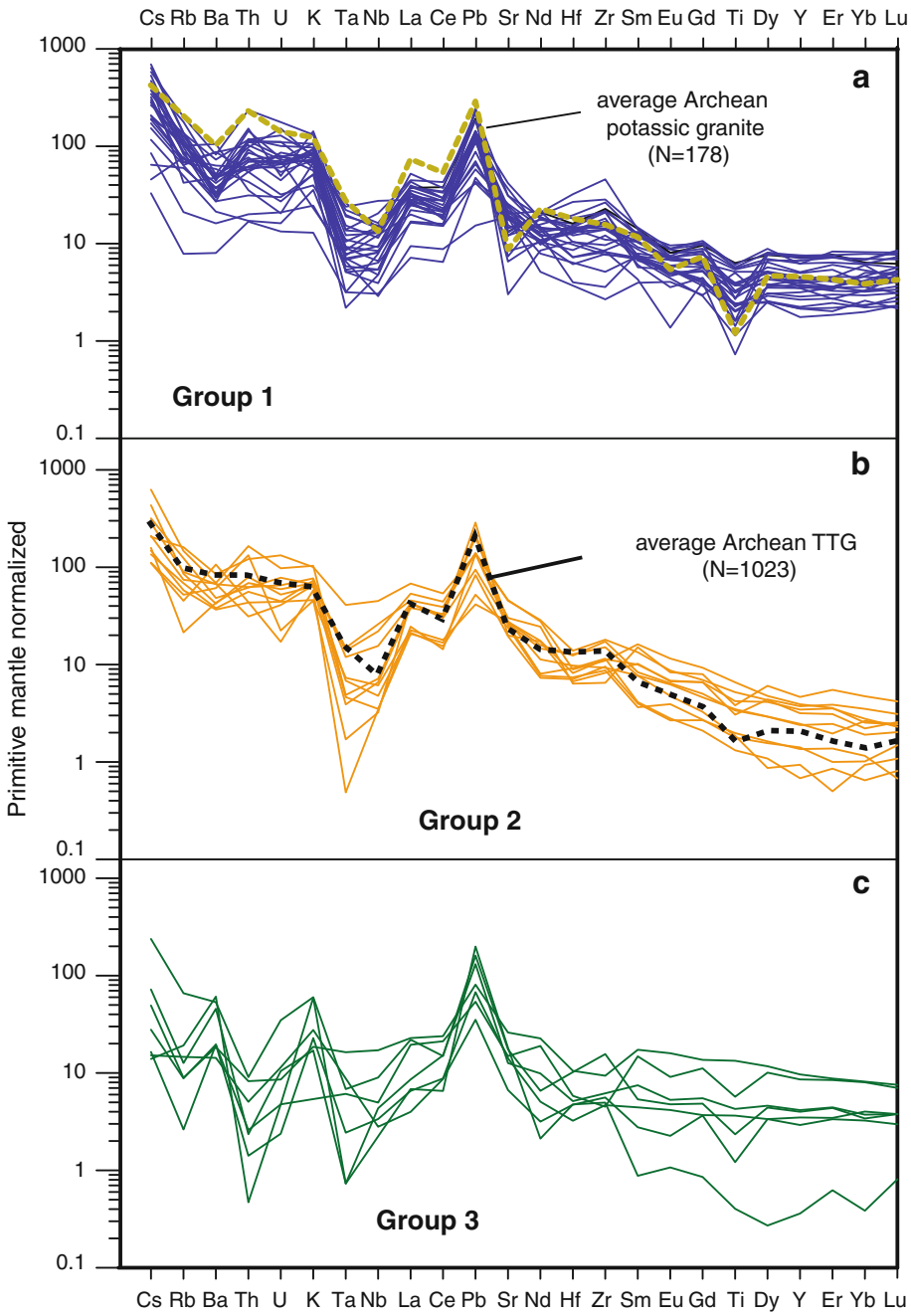

Fig. 7 Primitive mantle-normalized multi-trace-element patterns (Mcdonough and Sun 1995) of the Kohistan batholith granitoids. Group 1 (*top panel*) has enriched incompatible elements and unfractionated MREE/HREE. Contrary Group 2 (*middle panel*) has similar enriched incompatible element but fractionated MREE/HREE. Group 3 (*bottom panel*) has relatively unenriched incompatible elements and strongly fractionated Th/U. Group 1 and 2 are compared to averaged Archean GG- and TTG-type rocks, respectively (source same as Fig. 6)

Kohistan has taken place at the Nanga Parbat syntaxis. The exhumation of the Kohistan batholith started at ~50 Ma and was initiated by the India–Kohistan collision (van der Beek et al. 2009).

Correspondence of barometric pressures and actual crystallization depths

An excellent agreement exists between the constrained intrusion pressures, the observed igneous phase relationships between amphibole, epidote and plagioclase and experimental results that constrain the depth relationships of the relative crystallization sequence of the different minerals (Fig. 1). This strongly suggests that within the Kohistan batholith the recorded Al-in-hornblende pressures correlate with the magmatic emplacement depth. Also for the wider Kohistan arc, there is an excellent spatial continuity of igneous emplacement pressures (e.g., Al-in-hornblende) and metamorphic (re-)crystallization pressures (defined by net transfer reaction involving garnet), and a general agreement between the mapped thickness of various units and the petrologically constrained thickness exists (Jagoutz and Schmidt 2012). This indicates that the recorded pressures throughout the entire Kohistan arc are

close to the crystallization depths of the different intrusions. This finding has important implications for the growth mechanisms of the arc and indicates that burial of older rocks by subsequent emplacement of younger ones on top is of limited importance. This is in accordance with independent evidence for limited metamorphic burial (Yoshino and Okudaira 2004) and the dominance of isobaric cooling curves (Ringuette et al. 1999) in the deeper Kohistan crust.

Of significance for the crust-building process in arc batholiths are the extensive volumes of metavolcanic/metasedimentary rocks as, e.g., exposed near Jaglot, which are preserved in the Kohistan batholith throughout much of the middle and upper plutonic arc crust (Fig. 1). This so-called Jaglot group, composed of high-grade metasediments and metavolcanics (Khan et al. 2007; Yamamoto et al. 2011), strikes orthogonal to the isobars. In principle, the Jaglot group could represent a tectonic slice emplaced onto the Kohistan batholith during exhumation, but evidence for any thrusts or faults is absent. Instead, where contacts could be observed, they are primary magmatic, suggesting that the Jaglot group has been intruded by the batholith (Khan et al. 2007). The Jaglot group and similar smaller-scale metasedimentary/metavolcanic units are thus probably large fragments of initially surface rocks now situated at mid-crustal levels similar to what is observed in the Sierra Nevada batholith (Saleeby et al. 2003).

The absence of depth-dependent compositional variations in the Kohistan batholith

We use our dataset to investigate whether the chemical composition of a ~30-km-thick batholith varies systematic with depth. In order to extend the dataset for which direct pressure determination was possible, we interpolated the existing pressure estimates using a kriging routine incorporated into ArcMap (see Jagoutz 2013 for details). In Fig. 8 we plot the chemical composition of the Kohistan batholith granitoids against intrusion depth. A somewhat surprising but very apparent result is that no significant relationship exists between intrusion pressures and granitoid chemistry, neither in the major element composition of the intrusives (Fig. 8), nor in their trace element contents. The entire range of the compositional spectrum of the Kohistan batholith is observed at any depth from 8 to 30 km (Fig. 8). There is also no systematic association between intrusion pressure and trace element characteristics of the different groups, with the exception of Group 3 intrusives, which occur dominantly in spatial association with the Chilas Complex and therefore at the higher pressure end of the Kohistan batholith.

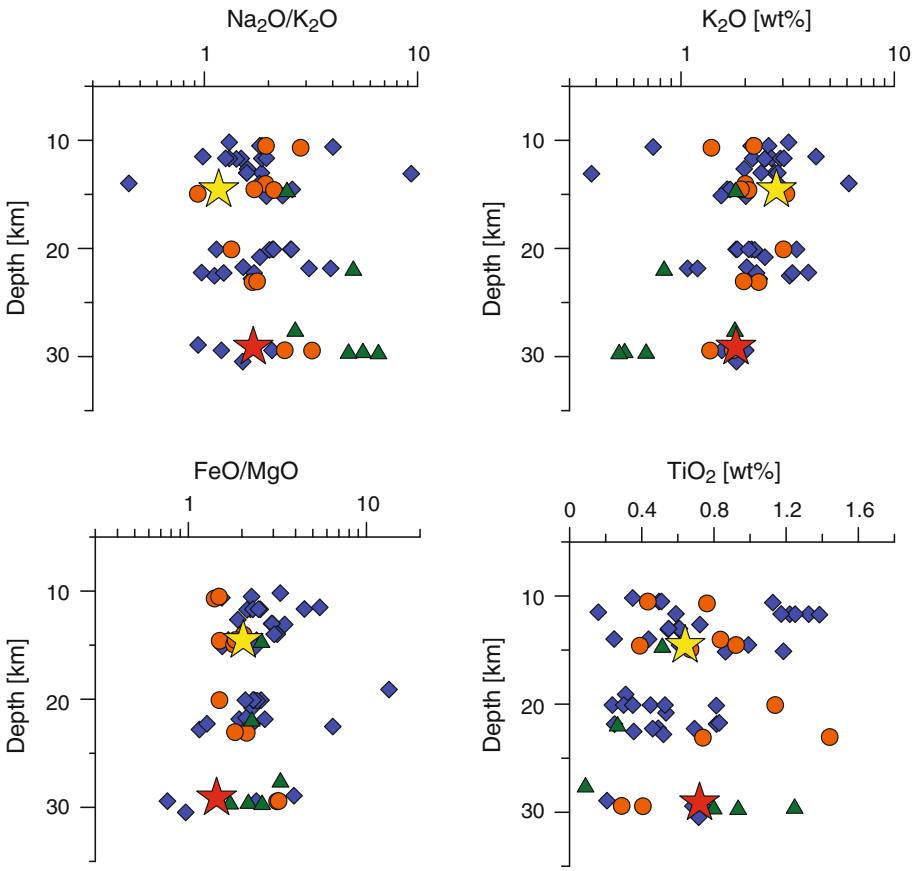

Fig. 8 Whole-rock chemical variation in the Kohistan batholith granitoids against emplacement depth (pressure converted assuming $\rho = 2{,}800$ kg/m^3). The different groups are based on the trace element characteristics of the whole rocks (see Fig. 7). Large variations in the chemical compositions are observed throughout the Kohistan batholith, yet no significant systematic chemical variation with depth is observed in the uppermost ~30 km of the plutonic crust of the Kohistan arc. *Symbols* as in Fig. 6

The role of magma mixing and magma mingling

Based on the studies of melt inclusions in volcanic rocks, it has been proposed that magma mixing in the deeper arc crust, between a more felsic and more mafic liquids, is an essential process to produce intermediate liquid compositions (e.g., Reubi and Blundy 2009). Our field observations (Figs. 2, 3) indicate indeed that magma mingling at all scales, between more mafic and more felsic melts, is a common process. However, we have never observed convincing evidence in the field that two magmas mingle and ultimately mix to form an intermediate composition. Melts with similar SiO_2 content (e.g., granodiorite/diorite or granodiorite/granite compositions) do not mix, and the compositional contact between different magmas remains sharp on a centimeter scale. As can be seen in, e.g., Fig. 2b, melts of different composition and viscosities remain separated even under high strain related to magmatic flow in small conduits. Similarly, Jagoutz (2010) has shown based on geochemical arguments (e.g., SiO_2 vs. TiO_2, etc.) that magma mixing is an inadequate process to explain the intermediate plutonic rock compositions observed in the Kohistan batholith. Therefore, we speculate that if magma mixing is indeed an essential process in producing intermediate volcanic compositions, it must occur at a level not included in our study area. For example, it is possibly that magma mixing is important in shallow-level subvolcanic magma chambers or during the eruption process itself.

Origin of the Kohistan batholith granitoids

The origin of I-type granitoids in arcs is very much discussed, and proposed models can be grouped in two end-member processes: partial melting of amphibolites in the lower arc crust (e.g., Clemens 1990; Clemens and Vielzeuf 1987; Tatsumi et al. 2008, 2009) or hydrous high- to medium-pressure magma differentiation with limited amount of assimilation in the lower crust (e.g., Davidson et al. 2007; Jagoutz et al. 2009; Sisson et al. 2005). We have previously discussed the origin of the Kohistan arc granitoids based on a more limited dataset and from the perspective of processes in the lower arc crust exposed in the Southern Plutonic Complex and the Chilas Complex (Jagoutz 2010; Jagoutz et al. 2009, 2011). In this context, the most important result is that two "separate" liquid lines of descent form the arc crust, a concept mirroring the already championed two melting regimes in the subarc mantle (Grove et al. 2002; Sisson and Bronto 1998): A more hydrous fractionation sequence, produced by relatively hydrous melts derived from flux melting, results in the formation of volumetrically important silica-rich granitoids controlled by either amphibole-dominated fractionation at medium pressures or garnet + hornblende at higher pressures (>0.8 GPa). The second liquid line of descent, produced by a less hydrous fractionation sequence related to decompression melting in the subarc mantle, results only in volumetrically minor granitoids and forms dominantly the basaltic lower crust preserved in arcs.

Chemical model of magma differentiation

The significant advantage of the Kohistan arc with respect to any other arc is the preservation of deeper arc units in the Southern Plutonic Complex that have trace element characteristics complementary to those observed in the middle to upper-crust granitoids. Based on this observation and a quantitative fractionation model, it has been shown that the Southern Plutonic Complex and the Kohistan batholith are related through a common differentiation process (Jagoutz 2010). In this differentiation model, the evolution of a parental melt is calculated by integrating actual rock compositions from the lower Kohistan arc crust. The cumulates evolve in composition from dunite (3 %), wehrlite (7 %), websterite (7 %), hornblendite/garnetite (10 %), gabbro (23 %), diorite (34 %) to cumulative tonalite (3 %) and are fractionated in seven steps from a primitive basaltic magma to finally arrive at a granite liquid. The numbers in brackets indicate the volume percentage of each cumulate type that has been fractionated; these volumes have been constrained from field observations and the mineral chemistry of these cumulates (see Jagoutz 2010 for details). This chemical model is a priori independent from the formation mechanism that formed the residual rocks (e.g., fractional or in situ crystallization, magma mixing, assimilation, melt–rock reaction, etc.). Nevertheless, petrological and geochemical studies on the different mafics and ultramafics in the lower Kohistan arc crust (Jagoutz et al. 2011) indicate that these are mostly cumulates formed from accumulation of magmatic crystals and subsequent incomplete extraction of interstitial liquids. Consequently, hydrous crystal fractionation was the dominant process in the lower arc crust, but this does not exclude a contribution from other magmatic processes such as magma mixing, assimilation or minor partial melting in the lower arc crust. Indeed, and as described above, fine-grained mafic enclaves within the granitoids of the Kohistan batholith are common and are generally interpreted as the results of magma mingling and mixing yet, we have not observed a single case where mingling of two magmas resulted in a homogenous intermediate composition.

Origin of the different granitoid groups: liquid lines of descent and parental magmas

One major finding in the extended dataset presented here relates to the presence of previously unrecognized three

different granitoid groups that have complementary cumulate compositions preserved in the lower arc crust.

The trace element systematics of the volumetrically dominant Group 1 granitoids, e.g., the concave MREE to HREE patterns and the negative Ti anomaly, is complementary to hornblendites at the base of the arc crust that have convex MREE to HREE and a positive Ti anomaly (Figs. 9, 10). The Group 1 granitoids can be modeled by fractionating minor volumes of hornblendite (Fig. 10) during hydrous medium- to high-pressure differentiation of primitive basaltic arc magmas. It is noteworthy that fluid-absent melting of mafic compositions would form clinopyroxene-dominated residues and not hornblendites, as hornblende is the major reactant in the fluid-absent melting reaction (Vielzeuf and Schmidt 2001).

Hornblendite dykes and lenses are abundant throughout the entire lower part of the arc (Burg et al. 2005), whereas garnetites (composed of garnet, clinopyroxene and minor hornblende) intercalated with hornblendites (composed of hornblende, clinopyroxen and minor garnet) are mostly restricted to a 1–2-km-thick layer at the base of the arc. Field and textural relationships in concert with the geochemical characteristic of the cumulate whole rocks indicate that these rocks are magmatic in origin. The cumulate compositions mimic the trace element characteristics of their constituent minerals, i.e., enrichment of HREE over MREE in the garnetites, compared to enrichment of MREE over HREE and LREE in the hornblendites (Fig. 9). The fact that garnetites are only observed in the lowermost part of the arc indicates a strong pressure control on their formation in agreement with the results from early-phase

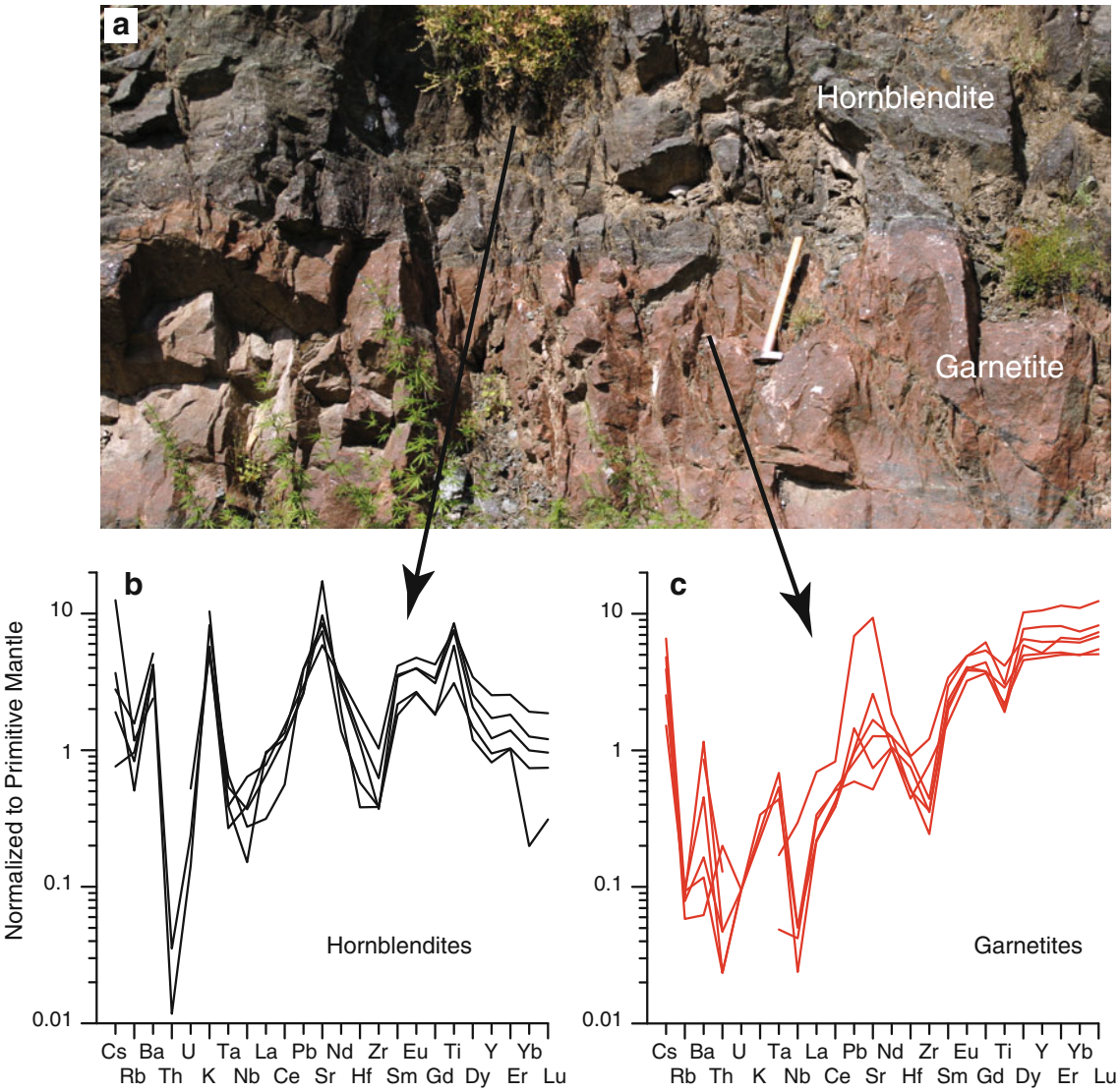

Fig. 9 Trace element concentrations and field occurrence (normalized to primitive mantle Mcdonough and Sun, 1995) of hornblendite (*left*, *black*) and garnetite (*right*, *red*) cumulates as preserved in the lowermost part of the arc (data after Dhuime et al. 2007; Jagoutz et al. 2011)

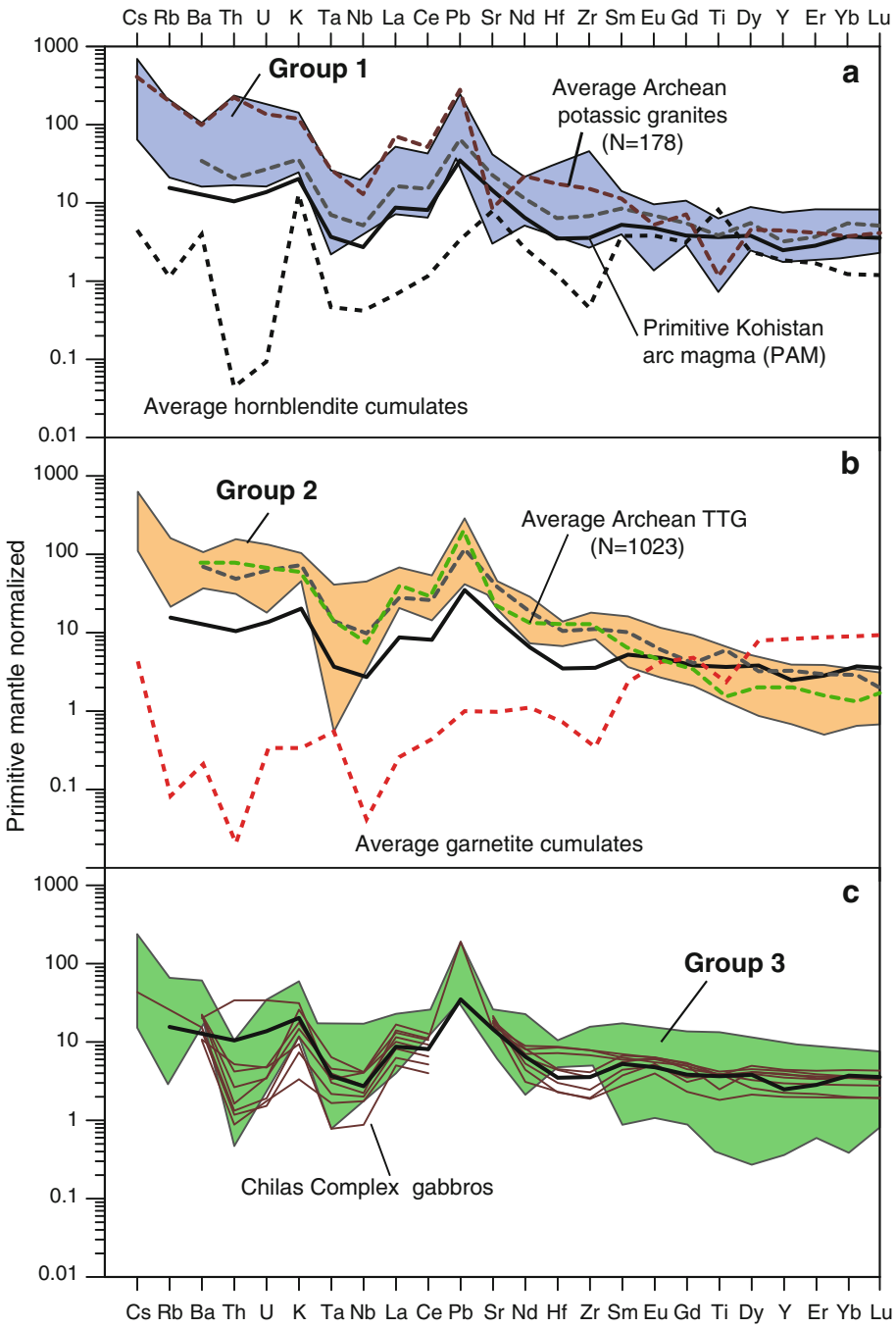

Fig. 10 Primitive mantle-normalized trace element plots. The uppermost *two panels* document the result of a fractionation model that explains the characteristics of the Group 1 and 2 rocks. Both groups have been modeled following the approach outlined in the text and in Jagoutz (2010). The trace element concentration of Group 1 rocks (*top panel*) can be modeled (*dashed gray line* representing ~90 % fractionation) as derived from an average Kohistan primitive arc magma (*blue line*) fractionating dunite (3 %), wehrlite (7 %), websterite (7 %), hornblendite (*dashed black line*, 10 %), gabbro (23 %), diorite (34 %) and cumulative tonalite (3 %). Similarly, Group 2 rocks (*middle panel*) can be modeled by fractionation as derived from a primitive arc melt (blue line) by fractionation of 3 % dunite, 7 % wehrlite, 7 % websterite, 10 % garnetite (*dashed red line*), 23 % gabbro, 34 % diorite and 3 % cumulative tonalite (*gray line* represents 90 % fractionation). Group 3 rocks (*bottom panel*) have similar trace element characteristics as the evolved rocks from the Chilas Complex (*brown lines*) that have been quantitatively modeled as formed by in situ crystallization of a anhydrous basaltic melt (see Jagoutz et al. 2006, 2007 for details)

diagram determinations (e.g., Lambert and Wyllie 1972) and from hydrous fractionation experiments (Alonso-Perez et al. 2009; Müntener et al. 2001). In these experiments garnet can be the sole or the dominant liquidus phase at high pressure (≥1.2 GPa) in andesitic to basaltic andesite liquids. An increase in H_2O content favors the stabilization of amphibole over garnet. At lower pressure (~0.8 GPa), amphibole is the dominant liquidus phase and garnet fractionates only at ~50–100 °C lower temperatures. We thus interpret the garnetite/hornblendite layers at the base of the arc as formed by hydrous magma differentiation from basaltic-andesitic liquids with variable H_2O content at high pressure. The hornblendite-only bodies in the shallower lower crust are the result of medium-pressure hydrous fractionation.

In an alternative interpretation of the SPC lower arc crust, Garrido et al. (2006) considered the garnetite and the garnet gabbro as the result of amphibole dehydration reactions, but ignores and hence fails to explain the hornblendites present therein across the entire lower Kohistan arc crust. As discussed by Jagoutz and Schmidt (2013), a number of field, petrological and geochemical

observations are not in accordance with this interpretation, and the interested reader is referred to these publications for an in-depth discussion.

Based on these observations, we modeled Group 2 granitoids using the fractionation model of Jagoutz (2010) for Group 1 granitoids but included 10 % of garnetite instead of hornblendite to reproduce the trace element systematic of Group 2 granitoids (Fig. 10). Rocks with adequate trace element concentrations are produced after 70–90 vol% fractionation, resulting in volumetrically important amounts of granitoids. Furthermore, the modeled trace element characteristics of Group 2 granitoids are essentially identical to those observed in many Archean TTG gneisses, indicating that high-pressure hydrous fractionation of garnet-bearing lithologies in the lower arc crust could lead to the formation of TTG suites in accordance with the model proposed by Kleinhanns et al. (2003).

Group 3 granitoids have significantly lower incompatible trace element concentrations than Group 1 and 2 granitoids. These three- to fourfold lower incompatible element concentrations cannot be explained by a liquid line of descent similar to those that formed Group 1 and 2 granitoids, but likely relate to differences in the original parental magma composition. The trace element systematics of Group 3 granitoids is similar to evolved rocks from the Chilas Complex (Fig. 10), which originated from a less hydrous parent liquid through a less hydrous liquid line of descent (Jagoutz et al. 2011). Therefore, the most likely scenario is that the Group 3 granitoids derived from the Chilas parent melt. This primitive melt was formed during an extensional stage of the arc through decompression melting in a part of the mantle wedge (Jagoutz et al. 2011) that had a significant lower slab-derived component than that of the Southern Plutonic Complex and most of the batholith (i.e., Group 1 and 2 granitoids). This is corroborated by the fact that most Group 3 granitoids are samples in the vicinity of the Chilas Complex.

The role of H_2O on emplacement of granitoids

The observation that Group 3 granitoids are spatially related to the Chilas Complex, whereas melts derived from the hydrous fractionation sequence are widespread throughout the entire batholith implies a different mobility of hydrous compared to less hydrous derivative liquids. A possible explanation lies in the fact that the different initial H_2O contents of the melts parental to the less hydrous and more hydrous fractionation lines result in severely different viscosities of the derivative melts. In Fig. 11 we calculated viscosities employing the model of Giordano et al. (2008) for melt compositions from appropriate hydrous and anhydrous fractionation experiments (Alonso-Perez et al. 2009; Müntener et al. 2001; Villiger et al. 2004). Based on these calculations, the viscosity of the derivative melts starts to differ significantly at ~52–55 wt% SiO_2. Highly differentiated dry liquids are about two to three orders of magnitude more viscous than hydrous ones. Consequently, the low viscosities of derivative liquids from the hydrous sequence facilitate the separation of these liquids from their source region. In contrast, gabbronorites of the less hydrous fractionation line retain more easily their residual tonalitic to granodioritic liquids and thus correspond commonly to

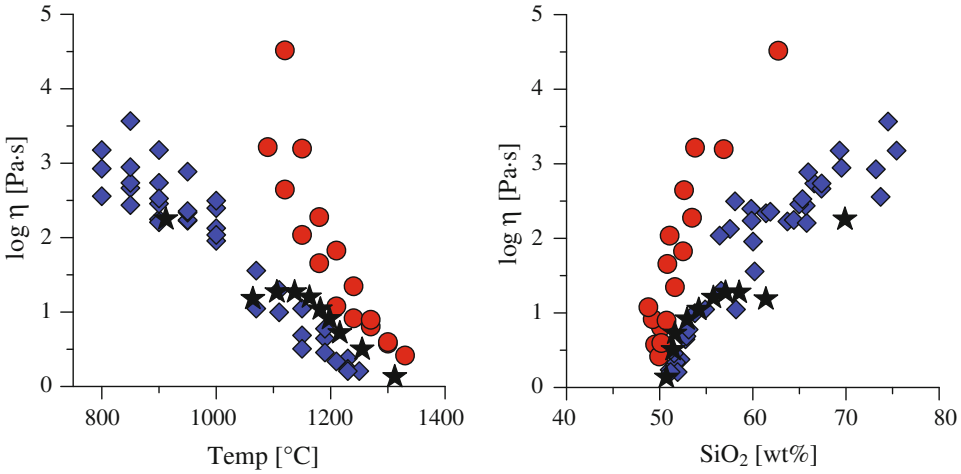

Fig. 11 *Left side* Calculated viscosities (using the model of Giordano et al. 2008) of hydrous (*blue*) and anhydrous (*red*) experimental liquids (Alonso-Perez et al. 2009; Müntener et al. 2001; Villiger et al. 2004) against liquidus temperature. *Stars* denote viscosities calculated for a hydrous LLD modified after the model of Jagoutz (2010). We assumed an initial H_2O content of 2 wt% and perfect incompatible behavior of the H_2O component. Liquidus temperatures for the modeled LLD were calculated at 0.8 GPa using MELTS (Ghiorso and Sack 1995). *Right side* The viscosity versus SiO_2 of the experimental and modeled liquids. The viscosity difference in derivative melts of a hydrous and anhydrous fractionation sequence becomes significant around 1,000–1,050 °C corresponding to ~52–55 wt% SiO_2

true melt compositions (Jagoutz et al. 2006, 2007). Consequently, the garnet- and hornblende-gabbros of the hydrous fractionation line are generally cumulative and do not correspond to true liquid compositions. Corroborating these different facilities of residual liquid extraction, the lower viscosity (and density) of the granitoids resulting from the hydrous fractionation line enhances their mobility when rising into the middle/upper arc crust.

Conclusions

The Kohistan arc batholith constitutes a complete section extending from shallow subvolcanic conditions to mid- to lower-crustal levels of ~30 km. Excluding minor peraluminous postcollisional granites, the batholith is dominantly composed of I-type granitoids that, based on their trace element systematics, can be grouped into three. The composition of the different granitoids groups is very similar to the Archean GG and TTG suites. For each of these groups, appropriate cumulate sequences are preserved in the lower arc crust. This lower arc crust complements the felsic granitoids to a basaltic primitive arc magma and documents that hydrous fractional crystallization is the dominant process forming the Kohistan batholith. Likely, a similar mechanism operated in the Archean. This observation questions the view that partial melting of the lower arc crust was dominant in forming TTG series.

Acknowledgments The study was supported by the Burri-Grubenmann foundation of IMP, ETH and the Albert Barth-Fund ETH to AE. OJ was supported by NSF EAR 6920005. We thank Peter Ulmer for help with the XRF analyses. Furthermore, we thank the people from Kohistan for their hospitality and kind assistance.

References

Ague JJ (1997) Thermodynamic calculation of emplacement pressures for batholithic rocks, California: implications for the aluminium-in-hornblende barometer. Geology 25(6):563–566

Alonso-Perez R, Müntener O, Ulmer P (2009) Igneous garnet and amphibole fractionation in the roots of island arcs: experimental constraints on H_2O undersaturated andesitic liquids. Contrib Miner Petrol 157:541–558

Anderson JL, Smith DR (1995) The effects of temperature and $F(O_2)$ on the Al-in-hornblende barometer. Am Mineral 80(5–6):549–559

Blundy JD, Holland TJB (1990) Calcic amphibole equilibria and a new amphibole-plagioclase geothermometer. Contrib Mineral Petrol 104(2):208–224. doi:10.1007/Bf00306444

Bouilhol P, Jagoutz O, Hanchar J, Dudas F (2013) Dating the India-Eurasia collision through arc magmatic records. Earth Planet Sci Lett 366:163–175

Burg JP (2011) The Asia–Kohistan–India collision: review and discussion. In: Arc-continent collision. Springer, Berlin, pp 279–309

Burg JP, Arbaret L, Chaudhry NM, Dawood H, Hussain S, Zeilinger G (2005) Shear strain localization from the upper mantle to the middle crust of the Kohistan Arc (Pakistan). In: Bruhn D, Burlini L (eds) High-strain zones: structure and physical properties, vol 245. Geological Society, London, pp 25–38

Burg JP, Jagoutz O, Hamid D, Hussain S (2006) Pre-collision tilt of crustal blocks in rifted island arcs: structural evidence from the Kohistan Arc. Tectonics 25(5):13. doi:10.1029/2005TC001835

Chappell B, White A (1992) I-and S-type granites in the Lachlan Fold Belt. Trans R Soc Edinb Earth Sci 83(1):26

Clemens JD (1990) The granulite-granite connexion. In: Vielzeuf D (ed) Granulites and crustal evolution. Kluwer, Dordrecht, pp 25–36

Clemens JD, Vielzeuf D (1987) Constraints on melting and magma production in the crust. Earth Planet Sci Lett 86(2–4):287–306

Condie KC (1993) Chemical composition and evolution of the upper continental crust: contrasting results from surface samples and shales. Chem Geol 104(1–4):1–37

Condie KC (1997) Plate tectonics and crustal evolution. Butterworth-Heinemann, Newton

Davidson J, Turner S, Handley H, Macpherson C, Dosseto A (2007) Amphibole "sponge" in arc crust? Geology 35(9):787–790

Dhuime B, Bosch D, Bodinier JL, Garrido CJ, Bruguier O, Hussain SS, Dawood H (2007) Multistage evolution of the Jijal ultramafic-mafic complex (Kohistan, N Pakistan): implications for building the roots of island arcs. Earth Planet Sci Lett 261:179–200

Drummond MS, Defant MJ (1990) A Model for Trondhjemite–Tonalite–Dacite genesis and crustal growth via slab melting—archean to modern comparisons. J Geophys Res Solid Earth Planets 95(B13):21503–21521

Dufek J, Bergantz GW (2005) Lower crustal magma genesis and preservation: a stochastic framework for the evaluation of the basalt–crust interaction. J Petrol 46(11):2167–2195

Garrido CJ, Bodinier JL, Burg JP, Zeilinger G, Hussain SS, Dawood H, Chaudhry MN, Gervilla F (2006) Petrogenesis of mafic garnet granulite in the lower crust of the Kohistan paleo-arc complex (northern Pakistan); implications for intra-crustal differentiation of island arcs and generation of continental crust. J Petrol 47(10):1873–1914

Ghiorso MS, Sack RO (1995) Chemical mass-transfer in magmatic processes. 4. A revised and internally consistent thermodynamic model for the interpolation and extrapolation of liquid-solid equilibria in magmatic systems at elevated-temperatures and pressures. Contrib Miner Petrol 119(2–3):197–212

Giordano D, Russell JK, Dingwell DB (2008) Viscosity of magmatic liquids: a model. Earth Planet Sci Lett 271(1–4):123–134

Green T (1972) Crystallization of calc-alkaline andesite under controlled high pressure hydrous conditions. Contrib Mineral Petrol 34:150–166

Green T (1982) Anatexis of mafic crust and high pressure crystallization of andesite. In: Thorpe RS (ed) Andesites: orogrenic andesites and related rocks. Wiley, New York, pp 465–487

Gromet P, Silver LT (1987) REE variations across the Peninsular Ranges batholith: implications for batholithic petrogenesis and crustal growth in magmatic arcs. J Petrol 28(1):75–125

Grove TL, Parman SW, Bowring SA, Price RC, Baker MB (2002) The role of an H_2O-rich fluid component in the generation of primitive basaltic andesites and andesites from the Mt. Shasta region, N California. Contrib Mineral Petrol 142(4):375–396

Hammarstrom JM, Zen E (1986) Aluminium in hornblende: an empirical igneous geobarometer. Am Mineral 71(3):1297–1313

Heuberger S, Schaltegger U, Burg JP, Villa IM, Frank M, Dawood H, Hussain S, Zanchi A (2007) Age and isotopic constraints on magmatism along the Karakoram-Kohistan Suture Zone, NW Pakistan: Evidence for subduction and continued convergence after India-Asia collision. Swiss J Geosci. doi:10.1007/s00015-007-1203-7

Holland T, Blundy J (1994) Nonideal interactions in calcic amphiboles and their bearing on amphibole-plagioclase thermometry. Contrib Mineral Petrol 116(4):433–447. doi:10.1007/Bf00310910

Hollister LS, Grissom G, Peters E, Stowell H, Sisson V (1987) Confirmation of the empirical correlation of Al in hornblende with pressure of solidification of calc-alkaline plutons. Am Mineral 72(3–4):231–239

Jagoutz O (2010) Construction of the granitoid crust of an island arc part II: a quantitative petrogenetic model. Contrib Mineral Petrol 160:359–381

Jagoutz O (2013) Were ancient granitoid compositions influenced by contemporaneous atmospheric and hydrosphere oxidation states? Terra Nova 25(3):95–101

Jagoutz O, Schmidt M (2012) The formation and bulk composition of modern juvenile continental crust: the Kohistan arc. Chem Geol 298–299:79–96

Jagoutz O, Schmidt MW (2013) The nature and composition of the crustal delaminate in arcs. Earth Planet Sci Lett 371–372:177–190. http://dx.doi.org/10.1016/j.epsl.2013.03.051

Jagoutz O, Müntener O, Burg J-P, Ulmer P, Jagoutz E (2006) Lower continental crust formation through focused flow in km-scale melt conduits: the zoned ultramafic bodies of the Chilas Complex in the Kohistan Island arc (NW Pakistan). Earth Planet Sci Lett 242(3–4):320–342

Jagoutz O, Müntener O, Ulmer P, Burg J-P, Pettke T (2007) Petrology and mineral chemistry of lower crustal intrusions: the Chilas Complex, Kohistan (NW Pakistan). J Petrol 48(10):1895–1953

Jagoutz O, Burg J-P, Hussain S, Dawood HTP, Iizuka T, Maruyama S (2009) Construction of the granitoid crust of an island arc part I: geochronological and geochemical constraints from the plutonic Kohistan (NW Pakistan). Contrib Mineral Petrol 158(6):739–755

Jagoutz O, Muentener O, Schmidt MW, Burg JP (2011) The respective roles of flux- and decompression melting and their relevant liquid lines of descent for continental crust formation: evidence from the Kohistan arc. Earth Planet Sci Lett 303:25–36

Johnson MC, Rutherford MJ (1989) Experimental calibration of the aluminium-in-hornblende geobarometer with application to Long Valley caldera (California) volcanic rocks. Geology 17(9):837–841

Khan MA, Jan MQ, Windley BF, Tarney J, Thirlwall MF (1989) The Chilas mafic-ultramafic igneous complex; the root of the Kohistan island arc in the Himalaya of northern Pakistan. In: Malinconico Lawrence L Jr, Lillie Robert J (eds) Tectonics of the western Himalayas, vol 232. Geological Society of America (GSA), Boulder, pp 75–94

Khan T, Murata M, Karim T, Zafar M, Ozawa H, Hafeez-ur-Rehman H (2007) A cretaceous dike swarm provides evidence of a spreading axis in the back-arc basin of the Kohistan paleo-island arc, northwestern Himalaya, Pakistan. J Asian Earth Sci 29(2–3):350–360. doi:10.1016/J.Jseaes.2006.04.001

Kleinhanns IC, Kramers JD, Kamber BS (2003) Importance of water for Archaean granitoid petrology: a comparative study of TTG and potassic granitoids from Barberton Mountain Land, South Africa. Contrib Mineral Petrol 145(3):377–389

Lambert IB, Wyllie PJ (1972) Melting of gabbro (quartz eclogite) with excess water to 35 kilobars, with geological applications. J Geol 80(6):693–708

Lambert IB, Wyllie PJ (1974) Melting of tonalite and crystallization of andesite liquid with excess water to 30 kilobars. J Geol 82:88–97

Leake BE (1978) Nomenclature of amphiboles. Am Mineral 63(11–12):1023–1052

Lee CTA, Morton DM, Kistler RW, Baird AK (2007) Petrology and tectonics of Phanerozoic continent formation: from island arcs to accretion and continental arc magmatism. Earth Planet Sci Lett 263(3–4):370–387

Martin H (1999) Adakitic magmas: modern analogues of Archaean granitoids. Lithos 46(3):411–429

McCulloch MT, Gamble JA (1991) Geochemical and geodynamical constraints on subduction zone magmatism. Earth Planet Sci Lett 102(3–4):358–374

Mcdonough WF, Sun SS (1995) The composition of the Earth. Chem Geol 120(3–4):223–253

Moyen JF (2011) The composite Archaean grey gneisses: petrological significance, and evidence for a non-unique tectonic setting for Archaean crustal growth. Lithos 123(1–4):21–36

Moyen J, Stevens G (2006) Experimental constraints on TTG petrogenesis: implications for Archean geodynamics. In: Benn K, Mareschal J-C, Condie KC (eds) Archean geodynamics and environments, vol 164. AGU, Washington, pp 149–175

Müntener O, Kelemen PB, Grove TL (2001) The role of H_2O during crystallization of primitive arc magmas under uppermost mantle conditions and genesis of igneous pyroxenites; an experimental study. Contrib Miner Petrol 141(6):643–658

Nawaz M, Hussain S, Qamar N, Ul-Islam Z, Akhtar J, Ur-Rehman S (1987) Geology and Petrography of Barawal-Dir-Bibior area. Geol Bull Punjab Univ 112:1543–1558

Petterson MG, Treloar PJ (2004) Volcanostratigraphy of arc volcanic sequences in the Kohistan arc, North Pakistan: volcanism within island arc, back-arc-basin, and intra-continental tectonic settings. J Volcanol Geother Res 130:147–178

Petterson MG, Windley BF (1985) Rb–Sr dating of the Kohistan arc-batholith in the trans-Himalaya of north Pakistan, and tectonic implications. Earth Planet Sci Lett 74(1):45–57

Petterson MG, Windley BF (1986) Petrological and geochemical evolution of the Kohistan arc-batholith, Gilgit, N. Pakistan. Geol Bull Univ Peshawar 19:121–149

Petterson MG, Windley BF (1991) Changing source regions of magmas and crustal growth in the trans-Himalayas; evidence from the Chalt Volcanics and Kohistan Batholith, Kohistan, northern Pakistan. Earth Planet Sci Lett 102(3–4):326–341

Reubi O, Blundy J (2009) A dearth of intermediate melts at subduction zone volcanoes and the petrogenesis of arc andesites. Nature 461(7268):1269–1273

Ringuette L, Martignole J, Windley BF (1999) Magmatic crystallization, isobaric cooling, and decompression of the garnet-bearing assemblages of the Jijal Sequence (Kohistan Terrane, western Himalayas. Geology (Boulder) 27(2):139–142

Rudnick R, Gao S (2003) The composition of the continental crust. In: Rudnick RL (ed) The crust, vol 3. Oxford, Elsevier, pp 1–64

Saleeby J, Ducea M, Clemens-Knott D (2003) Production and loss of high-density batholithic root, southern Sierra Nevada, California. Tectonics 22(6), art no 1064. doi:10.1029/2002tc001374

Schaltegger U, Zeilinger G, Frank M, Burg JP (2002) Multiple mantle sources during island arc magmatism, U–Pb and Hf isotopic evidence from the Kohistan arc complex, Pakistan. Terra Nova 14(6):461–468

Schmidt MW (1992) Amphibole composition in Tonalite as a function of pressure—an experimental calibration of the Al-in-hornblende barometer. Contrib Miner Petrol 110(2–3):304–310

Schmidt MW, Thompson AB (1996) Epidote in calc-alkaline magmas: an experimental study of stability, phase relationships, and the role of epidote in magmatic evolution. Am Mineral 81(3–4):462–474

Schmidt MW, Poli S (2004) Magmatic epidote. Rev Mineral Geochem 56(1):399–430. doi:10.2138/gsrmg.56.1.399

Sisson TW, Bronto S (1998) Evidence for pressure-release melting beneath magmatic arcs from basalt at Galunggung, Indonesia. Nature 391(6670):883–886

Sisson TW, Ratajeski K, Hankins WB, Glazner AF (2005) Voluminous granitic magmas from common basaltic sources. Contrib Miner Petrol 148(6):635–661

Smithies RH (2000) The Archaean tonalite–trondhjemite-granodiorite (TTG) series is not an analogue of Cenozoic adakite. Earth Planet Sci Lett 182(1):115–125

Streckeisen AL (1974) Classification and nomenclature of plutonic rocks. Recommendations of the IUGS subcommission on the systematics of igneous rocks. Geologische Rundschau. Internationale Zeitschrift für Geologie, Stuttgart 63:773–785

Sullivan MA, Windley BF, Saunders AD, Haynes JR, Rex DC (1993) A palaeogeographic reconstruction of the Dir Group; evidence for magmatic arc migration within Kohistan, N. Pakistan. In: Treloar PJ, Searle MP (eds) Himalayan tectonics, vol 74. Geological Society of London, London, pp 139–160

Tahirkheli RAK (1979) Geology of Kohistan and adjoining Eurasia and Indio-Pakistan continents, Pakistan. Geol Bull Univ Peshawar 11:1–30

Tamura Y, Gill JB, Tollstrup D, Kawabata H, Shukuno H, Chang Q, Miyazaki T, Takahashi T, Hirahara Y, Kodaira S, Ishizuka O, Suzuki T, Kido Y, Fiske RS, Tatsumi Y (2009) Silicic magmas in the Izu-Bonin Oceanic arc and implications for crustal evolution. J Petrol 50(4):685–723

Tatsumi Y, Shukuno H, Tani K, Takahashi N, Kodaira S, Kogiso T (2008) Structure and growth of the Izu-Bonin-Mariana arc crust: 2. Role of crust-mantle transformation and the transparent Moho in arc crust evolution. J Geophys Res 113(B2), art no B02203. doi:10.1029/2007jb005121

Thompson AB, Algor JR (1977) Model systems for anataxis of pelitic rocks.1. Theory of melting reactions in system $KalO_2$–$NalO_2$–Al_2O_3–SiO_2–H_2O. Contrib Miner Petrol 63(3):247–269

Treloar PJ, Rex DC, Guise PG, Coward MP, Searle MP, Windley BF, Petterson MG, Jan MQ, Luff IW (1989) K–Ar and Ar–Ar geochronology of the Himalayan collision in NW Pakistan; constraints on the timing of suturing, deformation, metamorphism and uplift. Tectonics 8(4):881–909

van der Beek P, Van Melle J, Guillot S, Pêcher A, Reiners PW, Nicolescu S, Latif M (2009) Eocene Tibetan plateau remnants preserved in the northwest Himalaya. Nat Geosci 2(5):364–368

Vielzeuf D, Schmidt MW (2001) Melting relations in hydrous systems revisited: application to metapelites, metagreywackes and metabasalts. Contrib Miner Petrol 141(3):251–267

Villiger S, Ulmer P, Muntener O, Thompson AB (2004) The liquid line of descent of anhydrous, mantle-derived, tholeiitic liquids by fractional and equilibrium crystallization—an experimental study at 1.0 GPa. J Petrol 45(12):2369–2388. doi:10.1093/Petrology/Egh042

Yamamoto H (1993) Contrasting metamorphic P–T-time paths of the Kohistan granulites and tectonics of the western Himalayas. J Geol Soc Lond 150(Part 5):843–856

Yamamoto H, Kobayashi K, Nakamura E, Kaneko Y, Kausar Allah B (2005) U–Pb zircon dating of regional deformation in the lower crust of the Kohistan Arc. Int Geol Rev 47:1035–1047

Yamamoto H, Rehman HU, Kaneko Y, Kausar AB (2011) Tectonic stacking of back-arc formations in the Thelichi section (Indus valley) of the Kohistan arc, northern Pakistan. J Asian Earth Sci 40(2):417–426

Yoshino T, Okudaira T (2004) Crustal growth by magmatic accretion constrained by metamorphic P–T paths and thermal models of the Kohistan arc, NW Himalayas. J Petrol 45:2287–2302

Yoshino T, Yamamoto H, Okudaira T, Toriumi M (1998) Crustal thickening of the lower crust of the Kohistan Arc (N. Pakistan) deduced from Al zoning in clinopyroxene and plagioclase. J Metamorph Geol 16(6):729–748